JPET Fast Forward. Published on August 16, 2019 as DOI: 10.1124/jpet.119.256792
This article has not been copyedited and formatted. The final version may differ from this version.

JPET # 256792

Withaferin A improves non-alcoholic steatohepatitis in mice

Daxesh P. Patel[1†], Tingting Yan[1†], Donghwan Kim[1], Henrique B. Dias[1,2], Kristopher W. Krausz[1], Shioko Kimura[1] and Frank J. Gonzalez[1*]

[1]Laboratory of Metabolism, Center for Cancer Research, National Cancer Institute, National Institutes of Health, Bethesda, Maryland, USA

[2]Laboratory of Cellular Biophysics and Inflammation, Pontifical Catholic University of Rio Grande do Sul, Brazil

[†]DPP and TY contributed equally to this study

JPET # 256792

Running Head: Withaferin A therapeutically improves NASH

***Corresponding author:** Frank J. Gonzalez, Laboratory of Metabolism, Center for Cancer Research, National Cancer Institute, National Institutes of Health, Bethesda, Maryland 20892, USA. Email: gonzalef@mail.nih.gov

Number of text pages: 31

Number of tables: 1

Number of figures: 13

Number of supplemental figures: 3

Number of references: 39

Words in Abstract: 222

Words in Introduction: 761

Words in Discussion: 1337

Section assignment for table of contents: Drug Discovery and Translational Medicine

ABBREVIATIONS: ALT, alanine aminotransferase; AST, aspartate aminotransferase; Cer, ceramide; H & E, hematoxylin and eosin; HFD, high-fat-diet; LFD, low-fat-diet; MCD, methionine-choline-deficient; MCS, methionine-choline-sufficient; NAFLD, non-alcoholic fatty liver disease; NASH, non-alcoholic steatohepatitis; NEFAs, non-esterified fatty acids; NRF2, nuclear factor erythroid 2-related factor 2; WA, withaferin A; TC, total cholesterol; TG, triglycerides. *Tnfa*, tumor necrosis factor alpha; *Il1b*, interleukin 1b; *Il6*, interleukin 6; *Hspa5*, heat shock protein family A (*Hsp70*) member 5; *Didt3,* DNA damage-inducible transcript 3*;*

Srebp1c, sterol regulatory element-binding protein 1c; *Fas*, fatty acid synthase; *Scd1*, stearoyl-CoA desaturase-1. *Timp2*, tissue inhibitor of metalloproteinase 2; *Col1a1*, collagen type I alpha 1; *Mmp2*, matrix metalloproteinase 2; *Acta2*, alpha smooth muscle actin; *Sptlc*, serine palmitoyltransferase, long-chain base subunit; *Smpd*, sphingomyelin phosphodiesterase; *Acer*, alkaline ceramidase; *Sgms*, sphingomyelin synthase; *Cers*, ceramide synthase; *NLRP3,* NLR family pyrin domain containing 3; *Gapdh,* glyceraldehyde 3-phosphate dehydrogenase; *Actb,* β-actin.

Abstract

Non-alcoholic steatohepatitis (NASH) is the progressive stage of non-alcoholic fatty liver disease (NAFLD) that highly increases the risk of cirrhosis and liver cancer, and there are few therapeutic options available in the clinic. Withaferin A (WA), extracted from the ayurvedic medicine *Withania Somnifera,* has a wide range of pharmacological activities, however, little is known about its effects on NASH. To explore the role of WA in treating NASH, two well-defined NASH models were employed, the methionine-choline-deficient (MCD) diet and the 40 kcal% high-fat diet (HFD). In both NASH models, WA treatment or control vehicle was administered to evaluate its hepatoprotective effects. As assessed by biochemical and histological analyses, WA prevented and therapeutically improved liver injury in both models, as revealed by lower serum aminotransaminases, hepatic steatosis, liver inflammation and fibrosis. In the HFD-induced NASH model, both elevated serum ceramides and increased hepatic oxidative stress were decreased in the WA-treated group compared to the control vehicle-treated group. To further explore whether WA has an anti-NASH effect independent of its known action in leptin signaling during combating obesity, leptin signaling-deficient ob/ob mice maintained on a HFD were employed to induce NASH. WA was also found to therapeutically reduce NASH in HFD-treated leptin-deficient ob/ob mice, thus demonstrating a leptin-independent hepatoprotective effect. This study revealed that WA treatment could be a therapeutic option for NASH treatment.

Keywords: Withania Somnifera; herb; hepatic steatosis; NASH; anti-oxidant

JPET Fast Forward. Published on August 16, 2019 as DOI: 10.1124/jpet.119.256792
This article has not been copyedited and formatted. The final version may differ from this version.

Introduction

Nonalcoholic steatohepatitis (NASH) is the progressive stage of nonalcoholic fatty liver disease (NAFLD) that results in a high risk of the end-stage liver diseases, cirrhosis and hepatocellular cancer (Farrell and Larter, 2006; Michelotti et al., 2013). While virus-induced hepatitis has been sharply reduced with vaccine application and curative drugs (Scott et al., 2015; Flemming et al., 2017), there continues to be an increase in NAFLD incidence due to the rapid rise of obesity and diabetes (Wong et al., 2014; Estes et al., 2018). NASH is currently listed as the second leading cause of liver disease among adults awaiting liver transplantation in the United States (Wong et al., 2015) and is estimated to overtake hepatitis C virus infection as the leading cause of liver transplantation in the US in the coming decades (Oseini and Sanyal, 2017). Although some conventional therapies such as vitamin E and pioglitazone could improve steatosis and inflammation, few treatments that could significantly decrease fibrosis, one of the strongest indicators of liver damage caused by NASH, have been found (Cassidy and Syed, 2016; Oseini and Sanyal, 2017), indicating that while market-available drugs are mostly effective in treating hepatic steatosis, they have minimal effects on fibrosis associated with NASH. There are no current FDA-approved therapies for treating NASH, and the development of novel medical treatments is urgently needed.

Withaferin A (WA), is a steroidal lactone derived from the plant *Withania Somnifera* used in traditional ayurvedic medicine (Vanden Berghe et al., 2012). WA was originally used as an anti-tumor agent (Lee and Choi, 2016) and has other pharmacological properties including cardioprotective, anti-inflammation and anti-oxidant activities (Vanden Berghe et al., 2012). Recently, WA was demonstrated to be a leptin sensitizer with strong antidiabetic properties in mice that could decrease obesity-associated metabolic abnormalities including hepatic steatosis

JPET Fast Forward. Published on August 16, 2019 as DOI: 10.1124/jpet.119.256792
This article has not been copyedited and formatted. The final version may differ from this version.

(Lee et al., 2016). Several other studies demonstrate that WA has hepatoprotective activity as revealed by its ability to mitigate acetaminophen-induced acute liver injury (Jadeja et al., 2015; Palliyaguru et al., 2016) and alleviate bromobenzene-induced liver injury (Vedi and Sabina, 2016). Since obesity is usually associated with insulin resistance and fatty liver, the pharmacological potential of WA in treating NASH needs to be evaluated.

NAFLD/NASH is known to be caused by a hepatic overload of fatty acids, leading to the production of toxic lipids that could cause hepatic oxidative stress, inflammation, endoplasmic reticulum (ER) stress and cell death (Friedman et al., 2018). Among the toxic lipids, ceramides are signaling molecules that accumulate in the blood and tissues in animal models of metabolic diseases. High cellular levels of ceramides are correlated with inflammation, cell death, oxidative stress, ER stress and insulin resistance (Pagadala et al., 2012; Chaurasia and Summers, 2015). Thus, strategies that decrease ceramides could efficiently improve NAFLD and NASH (Kurek et al., 2014; Jiang et al., 2015; Xie et al., 2017). On the other hand, WA is known to suppress oxidative stress, evidenced by its nuclear factor erythroid 2-related factor 2 (NRF2)-dependent effect in alleviating acetaminophen-induced liver injury and its effect in inducing heme oxygenase (HO-1) expression in endothelial cells via activating NRF2 pathway (Vanden Berghe et al., 2012; Jadeja et al., 2015; Heyninck et al., 2016; Palliyaguru et al., 2016). Besides, WA is a known leptin sensitizer that could both leptin signaling-dependently and leptin signaling-independently reduce diet-induced obesity as reported previously (Lee et al., 2016). Although there is no conclusive evidence that leptin is of value for the treatment of NAFLD patients, leptin was suggested to have a potential role in benefiting NASH treatment, as revealed by that recombinant leptin administration showed a beneficial effect in hepatic steatosis in NAFLD patients with hyperleptinemia (Polyzos et al.,

2015) or lipodystrophy patients (Javor et al., 2005). However, whether WA modulates ceramides homeostasis and alleviates oxidative stress during treating NASH, and whether WA affects NASH dependent on its effect on leptin signaling are still not known.

In the present study, two widely-used NASH models, the methionine- and choline-deficient (MCD) diet and the high-fat diet (HFD) were firstly employed to evaluate the efficacy of WA in treating NASH. WA had both preventive and therapeutic effects in improving NASH, as revealed by significant decreases of serum aminotransferases, hepatic steatosis, inflammation, ER stress and fibrosis. In the HFD-induced NASH model, WA alleviated NASH-associated oxidative stress and lowered serum ceramide levels. By using leptin-deficient ob/ob mice maintained on a NASH-promoting HFD, we further demonstrated that WA had a therapeutic effect in improving HFD-induced NASH in ob/ob mice, suggesting an leptin-independent anti-NASH effect of WA. All the present results indicate that WA could be repurposed as a novel therapy in treating NASH patients.

Materials and Methods

Chemicals and Reagents. WA was purchased from ChromaDex (Irvine, CA). PeroxiDetect kit, superoxide dismutase kit, glutathione assay kit and dimethyl sulfoxide were purchased from Sigma Aldrich (MO, USA). Alanine aminotransferase (ALT) kits and aspartate aminotransferase (AST) kits were purchased from Catachem (CT, USA). Total cholesterol (TC), triglyceride (TG), and non-esterified fatty acids (NEFAs) kits were purchased from Wako Pure Chemical Industries (Osaka, Japan). Ceramides standards C16, C18, C20, C22, C24, C18:1, C24:1 were purchased from Avanti polar Lipids (Alabaster, AL). Rodent diets with 40 kcal% high-fat, 20 kcal% fructose and 2% cholesterol (HFD, Cat# D09100301 for C57BL/6N mice and Cat# D09100310 for ob/ob mice) and 10 kcal% fat control diet (LFD, Cat# D09100304) were purchased

JPET Fast Forward. Published on August 16, 2019 as DOI: 10.1124/jpet.119.256792
This article has not been copyedited and formatted. The final version may differ from this version.

from Research Diets (NJ, USA). Methionine and choline sufficient (MCS) diet and MCD diet were purchased from Dyets Inc (Bethlehem, PA, USA).

Drugs Preparation and Dosing. The WA stock solution was dissolved in dimethyl sulfoxide and frozen, and before use diluted with saline to generate the treatment doses (the final dimethyl sulfoxide percentage was the same for all final injection solutions). WA was injected intraperitoneally (0.1 ml/20 g mouse) at the doses indicated once per day before the dark cycle of the day.

Animal Studies. Age-matched 6- to 8-week-old C57BL/6N males were housed in a specific pathogen-free environment controlled for temperature and light (25°C, 12-h light/dark cycle) and humidity (45-65%). The National Cancer Institute Animal Care and Use Committee approved all animal experiments conducted in this study. The mice were administered WA at a dose of 1 mg/kg, 2.5 mg/kg and 5 mg/kg for the MCD model and at the dose of 5 mg/kg for the HFD models. To test the preventative effect of WA in treating MCD-induced NASH, the mice were randomly divided into six groups: (1), MCS: mice fed the MCS diet and treated with control vehicle; (2), MCS+WA5: mice fed the MCS diet and treated with 5 mg/kg of WA; (3), MCD: mice fed the MCD diet and treated with control vehicle; (4), MCD+WA1: mice fed the MCD diet and treated with 1 mg/kg of WA; (5) MCD+WA2.5: mice fed the MCD diet and treated with 2.5 mg/kg of WA; (6) MCD+WA5: mice fed the MCD diet and treated with 5 mg/kg of WA. All mice were fed the MCS or MCD diets for four weeks, and WA or control vehicle was injected once per day from the first day of diet feeding. To test the therapeutic effect of WA in treating MCD diet-induced NASH, the mice were fed with the MCD diet for 6 weeks and then injected with WA once a day at the dose of 5 mg/kg during the last two weeks of MCD feeding. To test the preventive and therapeutic effect of WA in HFD-induced NASH model, mice were fed a HFD or LFD for 20

JPET Fast Forward. Published on August 16, 2019 as DOI: 10.1124/jpet.119.256792
This article has not been copyedited and formatted. The final version may differ from this version.

weeks. Mice were fed a HFD or LFD for 8 weeks and then divided into 4 groups; (1) mice treated with vehicle for 12 weeks; (2) mice treated with WA for 12 consecutive weeks; (3) mice treated with vehicle for 4 weeks from week 9 to week 12, and then treated with WA for the last 8 weeks; (4) mice treated with vehicle for 8 weeks from week 9 to week 16 and then treated with WA for 4 weeks. To test the therapeutic effect of WA in leptin-deficient NASH, the leptin-deficient ob/ob NASH mouse model was employed. Eight-week-old age-matched ob/ob mice, obtained from Jackson Laboratories, were fed a HFD for 8 weeks and then divided into two groups: (1) mice maintained on a HFD and treated with WA or control vehicle for 4 weeks; (2) mice maintained on a HFD and treated with WA for 4 weeks. The mice were injected with vehicle or WA before the dark cycle of the day and not fasted during the study. One hour after the last injection of WA or control vehicle, the mice were killed with CO_2 and serum and tissues collected for further analysis.

Histology Analysis. Formalin-fixed liver tissues were embedded in paraffin. A portion of fresh livers were embedded in Tissue-Tek Optimal Cutting Temperature compound (Sakura Finetek, Torrance, USA) and then flash frozen for Oil Red O staining. Five μm thick sections were cut for both H&E and picrosirius red staining. Further sample processing, and analysis for H&E staining, and Oil red O staining were performed at Histoserv Inc (Germantown, MD, USA) or VitroVivo Biotech (Rockville, MD, USA). For picrosirius staining in Figure 8, paraffin-embedded livers were sectioned at Histoserv Inc and stained with picrosirius based on its manual, while picrosirius staining for Figure 12 were performed in VitroVivo Biotech (Rockville, MD, USA). Digital images from picrosirius red-stained liver sections were analyzed with ImagePro plus software (Media Cybernetics, Inc., Rockville, MD, USA), and the collagen positive area was assessed. Large blood vessels and corner sections were excluded from analysis and at least five different fields of each slide were measured to allow a realistic picture of the entire organ's fibrotic

state. Results were expressed as collagen percentage of all images related to the total area of the tissue.

Biochemical Analysis of Liver and Serum. Biochemical parameters including levels of ALT, AST, TC, TG and NEFAs, as well as levels of superoxide dismutase, hydroxide peroxide and glutathione in serum or liver were tested with commercial kits based on the manuals. Serum ceramides were quantified as described previously (Xie et al., 2017).

Quantitative Polymerase Chain Reaction. The livers were flash frozen in liquid nitrogen and stored at -80°C. Total RNA from frozen livers was extracted with TRIzol reagent (Invitrogen, Carlsbad, CA). cDNA was synthesized from 1 μg of total RNA using qScript cDNA SuperMix (Gaithersburg, MD). Analysis was performed by using the ABI PRISM 7900 Sequence Detection System (Applied Biosystems, Bedford, MA). Values were normalized to *Actb* or *Gapdh* mRNAs and the results expressed as fold change relative to the control group. Primer sequences are listed in Supplementary table 1.

Pharmacokinetic Analysis. Age and body weight-matched 8-week-old C57BL/6N mice were randomly-grouped and dosed with 5 mg/kg of WA via intraperitoneal administration. Blood was collected at 0 min (pre-dose), 10 min, 20 min, 40 min, 1 h, 2 h, 4 h, 8 h, 24 h and 48 h for isolation of plasma. Samples were diluted with acetonitrile and protein removed by centrifugation, and then analyzed using UPLC-MS/MS under reverse phase chromatography after optimizing chromatographic conditions for WA. MassLynx software version 4.1 was used to analyze the data of drug concentration. The pharmacokinetic parameters of WA were calculated by non-compartmental model using WinNonlin software version 5.2.1 (Pharsight Corporation, Sunnyvale, CA, USA). The C_{max} values and the time to reach maximum plasma concentration (T_{max}) were calculated directly from the observed plasma concentration vs time data. The area under the plasma

drug concentration–time curve from time 0-48h ($AUC_{0–48h}$) was calculated using the linear trapezoidal rule. The $AUC_{0–infinity}$ was calculated as: $AUC_{0–infinity}=AUC_{0–48h}+ C_t/K_{el}$, where C_t is the last plasma concentration measured and K_{el} is the elimination rate constant; K_{el} was determined using linear regression analysis of the logarithm linear part of the plasma concentration–time curve. The $t_{1/2}$ of WA was calculated as $t_{1/2}=ln2/K_{el}$.

Statistical Analysis. Experimental values were presented as mean ± SD. Statistical analyses were determined by two-tail t test between two groups or by one-way ANOVA followed by Dunnett's multiple comparisons test among multiple groups using Prism version 7.0 (GraphPad Software, San Diego, CA). P values less than 0.05 were considered statistically significant.

Results

WA Dose-dependently Attenuates MCD Diet-induced Liver Injury. To explore the effect and effective dose of WA in the MCD diet-induced liver injury model, WA at 1, 2.5, and 5 mg/kg were administered. From the first day of MCD diet feeding, WA was injected once a day for four consecutive weeks (Fig. 1A). The MCD diet induced body weight loss, which was significantly attenuated by WA at 5 mg/kg (Fig. 1B). WA dose-dependently increased the liver weight and liver index in mice on the MCD diet (Fig. 1, C and D). WA treatment alone caused no significant histologic changes indicating liver damage (Fig. 1E) and did not significantly affect serum ALT and AST levels (Fig. 2, A and B) in the control MCS diet feeding group, indicating that WA at 5 mg/kg was not hepatotoxic. Further biochemical assays showed that WA dose-dependently inhibited the MCD diet-induced increase of serum ALT and AST levels (Fig. 2, A and B) as well as hepatic levels of TC and TG (Fig. 2, C and D). The MCD diet induced a marked

decrease of serum TC and TG, which was significantly attenuated by 5 mg/kg WA (Fig. 2, E and F). Given that WA at 5 mg/kg, among the tested doses, showed a consistent effect in reversing body weight changes, serum ALT and AST levels, TC and TG levels in livers and serum, the effect of 5 mg/kg of WA in hepatic inflammation and histology were measured at this dose. WA alleviated MCD diet-induced liver inflammation (Fig. 2G), and histological analyses by H & E and Oil Red O staining showed that 5 mg/kg of WA improved MCD diet-induced hepatic steatosis (Fig. 2, H and I). These data demonstrate that WA dose-dependently prevents MCD diet-induced fatty liver, and that the 5 mg/kg dose of WA ameliorates NASH.

With a dose of 5 mg/kg WA chosen for further extensive study, a pharmacokinetic analysis was performed to investigate the exposure and clearance behavior of WA in blood after intraperitoneal injection. The chemical structure of WA and drug concentration-time curve of WA are shown (Supplemental Fig. 1, A and B). The pharmacokinetic parameters including $C_{max,}$ $T_{1/2}$, $AUC_{0–48h}$, $AUC_{0-\infty}$ and elimination rates ($K_{eli,}$ 1/h) were calculated (Supplemental Fig.1C). Following a single intraperitoneal injection dose of 5 mg/kg WA, a C_{max} level of 14.3 ± 1.8 nM was observed at 20 min. The plasma $T_{1/2}$ value of WA was 2.0 ± 0.6 h. These data and a previous study (Thaiparambil et al., 2011) that found intraperitoneally-injected WA had a half-life of 1.36 h, suggest that WA has a rapid clearance from blood after intraperitoneal dosing. However, WA was readily detected across the time-course of 48 h and was maintained at 2-4 nM (14%-29% percent of WA peak concentration) at the later phase after a single dose of 5 mg/kg WA (Supplemental Fig. 1B). These data suggest that WA could be maintained at a relatively low level for 48 h, while having a short half-life of 2 h in mice. However, its pharmacokinetics my differ in humans.

WA Prevents MCD Diet-induced Liver Injury Independent of Body Weight Change. To examine whether WA could prevent MCD diet-induced NASH independent of its effect in changing MCD diet-induced body weight loss, a short-term MCD diet feeding study was performed. Mice were fed an MCD diet for 10 days, during which 5 mg/kg of WA or control vehicle was injected once a day for 10 consecutive days (Fig. 3A). In this short-term study, 5 mg/kg of WA did not change the body mass of MCD diet-fed mice (Fig. 3B). However, WA markedly increased the liver weight and the liver index when compared with control vehicle-treated controls (Fig. 3, C and D). Five mg/kg of WA significantly decreased the MCD diet-induced serum ALT and AST levels (Fig. 3, E and F). These data demonstrate that 5 mg/kg WA is sufficient to alleviate MCD diet-induced liver injury at the early stage in the absence of significant body weight changes.

WA Therapeutically Improves MCD Diet-induced Liver Injury. To further explore whether WA could therapeutically treat MCD diet-induced NASH, 5 mg/kg WA was administered for two weeks after the onset of liver damage induced by 6 weeks of MCD diet feeding (Fig. 4A). WA did not affect the body weight, liver weight and liver index (Fig. 4, B-D), while it significantly decreased the MCD diet-induced increases of serum ALT and AST levels (Fig. 4, E and F). WA also improved hepatic steatosis as revealed by histological analyses (Fig. 4, G and H). These data suggest that 5 mg/kg WA therapeutically improves MCD diet-induced liver injury.

WA Improves HFD-induced Liver Injury. In contrast to the MCD diet-induced NASH model that results in body weight loss and does not cause insulin resistance coincident with inducing steatohepatitis, the 40 kcal% HFD-induced obese NASH model is thought to better mimic the typical human NASH pathologies of insulin resistance, high serum lipids accumulation and obesity (Hebbard and George, 2011; Griffett et al., 2015; Honda et al., 2016; Ding et al., 2018).

JPET Fast Forward. Published on August 16, 2019 as DOI: 10.1124/jpet.119.256792
This article has not been copyedited and formatted. The final version may differ from this version.

To further confirm the effect of WA in treating NASH, the HFD regimen and its matched LFD were used to test the effect of WA both in preventing and therapeutically improving NASH. Mice were fed a HFD for 20 weeks and injected with 5 mg/kg of WA or control vehicle for the last 12, 8, or 4 weeks before killing (Fig. 5A). WA significantly decreased body weights in both the HFD-fed and LFD-fed mice (Fig. 5, B and C). WA also decreased liver weights and liver indexes (Fig. 5, D and E) and attenuated the HFD-induced increase of serum ALT and AST (Fig. 5, F and G) in a time-dependent manner. Similarly, WA treatment decreased the HFD-induced accumulation of hepatic TG and TC levels (Fig. 6, A and B) and serum TG and TC levels (Fig. 6, C and D). WA treatment time-dependently decreased the HFD-induced accumulation of NEFAs in both livers and serum (Fig. 6, E and F). Further histological analyses showed that WA treatment time-dependently improved NASH-associated hepatic steatosis as revealed by histological analyses (Fig. 7, A and B). WA treatment also significantly reduced the levels of the HFD-induced *Tnfa, Il1b*, and *Il6* mRNAs involved in hepatic inflammation (Fig. 7, *C-E*) and heat shock protein family A member 5 (*Hspa5)* and DNA damage-inducible transcript 3 (*Ddit3)* mRNA levels involved in ER stress (Fig.7, *F* and *G*). WA treatment decreased the HFD-induced increase of *Srebp1c* mRNA encoding the transcription factor SREBP1C and its downstream target gene mRNAs, *Scd1* and *Fas* involved in the control of lipogenesis (Fig. 7, H-J). These data demonstrate that WA treatments both prevent and therapeutically improve HFD-induced hepatic steatosis, inflammation, and ER stress accompanied by dampening the hepatic lipogenesis signaling.

WA Attenuates Hepatic Fibrosis. Fibrosis is a major hallmark of NALFD progression to NASH. Twenty-week HFD feeding markedly induced picrosirius red staining in the NASH group, which was rescued by WA treatment in a time-dependent manner (Fig. 8A). Further statistical analysis showed that WA treatment decreased NASH-associated hepatic collagen accumulation

(Fig. 8B). In addition, WA treatment decreased *Timp2*, *Col1a1*, *Mmp2*, and *Acta2* mRNAs encoding enzymes and structural proteins involved in liver fibrogenesis (Fig. 8, *C*-*F*). These data demonstrate that WA improves NASH-associated fibrosis induced by HFD in a time-dependent manner.

WA Rescues NASH-associated Ceramide Accumulation, ER Stress and Oxidative Stress. Previous studies demonstrated that HFD-induced hepatic steatosis was correlated with increased ceramide levels (Longato et al., 2012; Chaurasia and Summers, 2015; Kasumov et al., 2015). Genetically or biochemically decreasing ceramides improved NAFLD and NASH (Kurek et al., 2014; Xie et al., 2017). Oxidative stress that occurs in NASH could induce ceramide accumulation (Bikman and Summers, 2011) and WA has exhibited anti-oxidant activity in earlier experimental models (Vanden Berghe et al., 2012). Thus, the anti-oxidant effects of WA could potentially influence ceramide levels and oxidative stress during treating NASH. To examine this hypothesis, levels of serum ceramides were first measured using authentic standards. HFD significantly induced the accumulation of ceramides, such as C16 (m/z 582.5098), C18 (m/z 610.5411), C20 (m/z 638.5724), C22 (m/z 666.6037), C24 (m/z 694.6350), C18:1 (m/z 608.5254), and C24:1 (m/z 692.6193), all of which were reduced by WA treatment (Fig. 9, *A*-*G*).

Next, that possibility that WA attenuated HFD-induced oxidative stress was examined. WA treatment time-dependently rescued the NASH-induced decrease of hepatic superoxide dismutase and glutathione levels, and significantly attenuated the NASH-induced increase of hepatic peroxide levels (Fig. 9, H-J). These data suggest that WA treatment reduces HFD-induced ceramides accumulation in serum and oxidative stress in liver.

To further examine why WA alleviated serum ceramides accumulation and hepatic oxidative stress, mRNA levels of ceramides signaling and NRF2 signaling were analyzed. WA

treatment markedly decreased mRNAs of genes involved in ceramide biosynthesis pathways, such as serine palmitoyltransferase, long-chain base subunit 1 (*Sptlc1)* and *Sptlc2*, sphingomyelin phosphodiesterase *1 (Smpd1)*, *Smpd2*, *Smpd3*, *and Smpd4*, angiotensin-converting enzyme-related *2 (Acer2)* and *Acer3*, sphingomyelin synthase (*Sgms1)* and *Sgms2*, ceramide synthase 2 (*Cers2)*, *Cers4* and *Cers6* in a time-dependent manner (Fig. 10, A-M). These data demonstrate that WA attenuates HFD-induced accumulation of serum ceramides and oxidative stress. Further analysis of NRF2 signaling revealed that WA decreased mRNA levels of genes involved in NRF2 pathway both in 20-week HFD-treated mice (Supplemental Fig. 2) and 4-week MCD diet-treated mice (Supplemental Fig. 3A). Given that earlier reports revealed that WA could activate NRF2 (Jadeja et al., 2015; Heyninck et al., 2016; Palliyaguru et al., 2016), the possibility exists that the decreases NASH diet-induced NRF2 signaling by WA in the current study is due to a secondary result of its hepatoprotective effects. The marked hepatoprotective effect may decrease NASH diet-promoted NRF2 signaling, which could overcome the effect of WA on NRF2 activation under that pathological conditions of NASH. To answer this question, the effect of WA in hepatic NRF2 signaling pathway at an early stage of NASH model induced by the MCD diet or HFD was examined. Mice were fed with an MCD diet for 10 days or a HFD for one week, during which mice were cotreated with control vehicle or 5 m/kg of WA once a day via intraperitoneal injection, and all mice were killed one hour after the last WA injection to collect livers for further mRNAs analysis. In 10-days MCD diet-fed mice, WA was found to induce hepatic mRNAs of NRF2 target genes including *Gclc, Nqo1*, *Keap1*, *Cat* and *Nrf2* (Supplemental Fig. 3B), while in one-week HFD-treated mice, this NRF2-activating effect of WA was not found. These data suggest that WA may affect the mRNAs expression of NRF2 target genes in a context-dependent manner.

JPET Fast Forward. Published on August 16, 2019 as DOI: 10.1124/jpet.119.256792
This article has not been copyedited and formatted. The final version may differ from this version.

WA Improves NASH in HFD-induced Liver Injury in Leptin Signaling Defective (ob/ob) Mice. To determine the effect of WA in a leptin-deficient NASH model, ob/ob mice were fed a HFD for 12 weeks and injected with 5 mg/kg of WA or control vehicle for the last 4 weeks before killing (Fig. 11A). WA significantly decreased body weight, the liver weight and liver index (Fig. 11, B, C and D), and attenuated the HFD-induced increase of serum ALT and AST (Fig. 11, E and F). Histological analyses revealed that WA treatment improved NASH-associated hepatic steatosis (Fig. 11, G and H). Consistent with this finding, WA treatment reduced the mRNA levels of proinflammatory cytokines including *Il1b*, *Il6* and *Tnfa* mRNAs, as well as the mRNA levels of lipogenesis genes including *Srebp1*c, *Scd1* and *Fas* (Fig. 11I). WA treatment decreased the HFD-induced accumulation of TG, TC and NEFAs in liver and serum (Fig. 12, *A-F*). Furthermore, WA also significantly reduced the mRNA levels of the fibrogenesis genes *Timp2*, *Col1a1*, *Mmp2* and *Acta2* (Fig. 12G) and attenuated HFD-induced hepatic fibrosis as revealed by picrosirius red staining data (Fig. 12H). Similar to its effect in HFD-treated C57BL/6N mice, WA also significantly decreased HFD-induced ER stress markers *Hspa5* and *Ddit3* mRNAs, as well as all the tested mRNAs involved in ceramide synthesis including *Sptlc1, Sptlc2*, *Smpd2*, *Smpd3*, *Acer2*, *Sgms1*, *Sgms2*, *Cers2*, *Cers4* and *Cers6* (Fig. 12, I and J). These results demonstrate that WA treatment decreases HFD-induced NASH in ob/ob mice, and this was in accompany by decreased hepatic ceramide synthesis.

Discussion

The hepatoprotective roles of WA in treating liver diseases, especially the effects on NASH are largely unknown. The current study revealed that WA could both prevent and therapeutically improve NASH in two well-defined mouse NASH models, MCD-induced NASH model and HFD-

induced NASH model in C57BL/6N mice and could therapeutically alleviate a leptin-deficient HFD-induced NASH model in ob/ob mice. WA restored NASH-induced dysregulation of oxidative stress and lowered ceramides that may be involved in the mechanism of NASH (Fig. 13). However, detailed mechanistic analysis required further studies.

The MCD diet-induced NASH model has been a widely-used for evaluating the pharmacological effects of drugs on NASH (Hebbard and George, 2011) and provides convenience for its short-term experimental duration. By using this rapid short-term model, the efficient dose of WA on NASH was found to be 5 mg/kg that was efficient in both preventing and therapeutically treating MCD diet-induced NASH. Compared with the MCD diet-induced lean NASH model, the HFD-induced NASH model more accurately reflects the clinical NASH pathologies including obesity, insulin resistance and high serum triglycerides, in addition to the typical hepatic steatosis, inflammation and fibrosis (Hebbard and George, 2011), and thus this model was chosen for further determining the effects of WA on NASH. In the obese NASH model, WA treatment improved NASH-associated pathologies including hepatic steatosis, inflammation and fibrosis in a time-dependent manner. Since HFD diet feeding causes hepatic steatosis and minor fibrosis after a two-month diet feeding that gradually progresses to advanced NASH (Ding et al., 2018), the effect of WA treatments for twelve weeks during the full course of HFD feeding would be mainly regarded as a preventive effect, while WA treatment for eight weeks and four weeks after the onset of NASH would evaluate the therapeutic effects. In addition to WA's effect in improving NASH, WA also decreased HFD-induced body weight gain, in agreement with its known anti-obesity activity (Lee et al., 2016). Whether the effect of WA is the result of its anti-obesity effect or a direct effect on NASH in the present HFD-induced NASH model still requires further study. By using the NASH-promoting HFD, the current study extends the pharmacological known effects of WA to improving

NASH, beyond its known effects on obesity-accompanied hepatic steatosis associated with its anti-obesity effect (Lee et al., 2016). However, weight loss caused by WA treatment could potentially ameliorate the HFD-induced NASH. Given that the body weight was sharply decreased upon WA treatment in the current HFD-induced fat NASH model as well as in the previous study (Lee et al., 2016), it would be difficult to separate the anti-obesity effect as the cause of decreased NASH as opposed to a direct pharmacological effect of WA on NASH. However, the MCD-induced NASH mice show lean body weight instead of obesity, and the inhibitory effect of WA on MCD diet-induced NASH suggests that WA has a direct hepatoprotective effect in treating NASH independent of obesity at least in this non-obese NASH model. As noted earlier, the present study provides evidence that WA potently improves MCD diet-induced NASH, a lean NASH mouse model, in which some hepatoprotective effects, such as the therapeutic effect of WA at the dose of 5 mg/kg on MCD-induced NASH and the preventive effect on MCD-induced NASH at doses of 1 mg/kg and 2.5 mg/kg, are independent of body weight change. Furthermore, WA could also markedly decrease MCD diet-induced increase of serum ALT and AST and increased liver weights prior to body weight changes after MCD diet feeding for ten days. Similar with the present finding, it was reported that the hepatoprotective component glycyrrhizin also reduced MCD diet-induced NASH without significantly affecting the MCD diet-induced body weight loss (Yan et al., 2018). On the other hand, WA was reported to therapeutically improve acetaminophen-induced acute liver injury even when injected 1 hour after acetaminophen dosing (Jadeja et al., 2015), indicating that WA has a direct hepatoprotective effect. The current work, together with previous studies, suggests that WA could improve NASH, at least potentially due to its direct hepatoprotective activity, independent of its anti-obesity effect.

WA was previously reported to act as a leptin-sensitizer during obesity and was also shown to exert an anti-obesity effect independent of leptin signaling, as WA still had an anti-obesity effect in leptin-deficient mice (Lee et al., 2016). Thus, the question arose whether the anti-NASH effect of WA was dependent on leptin signaling. Consistent with this previous study, WA still elicited a potent therapeutic effect in HFD-induced NASH in leptin-deficient ob/ob mice. Thus, WA has leptin-independent pharmacological activity in obesity and obesity-associated NASH.

In the present study, WA was found to reduce the accumulation of ceramides in serum accompanied with attenuation of HFD-induced upregulation of ceramides. WA also decreased hepatic oxidative stress and hepatic ER stress, which were correlated with its anti-NASH effects. Although all these analyses provide potential hints for further mechanism exploration, the study does not determine how WA directly affects oxidative stress signaling, ER stress signaling, ceramides signaling or stress-treated ceramides signaling. *In vitro* studies are warranted to answer this question. Previous studies demonstrate that WA has antioxidant activity via activating NRF2 (Cassidy and Syed, 2016; Palliyaguru et al., 2016) and anti-inflammatory potential via directing inhibiting NLR family pyrin domain containing 3 (NLRP3) inflammasome activation (Kim et al., 2015; Dubey et al., 2018). Although in the present study, WA attenuated NASH-induced NRF2 signaling at the terminal stages of the NASH model, which may be a result of its hepatoprotective effects, WA could activate NRF2 signaling in the early stages of NASH within 10-days of commencing MCD diet treatment, although WA did not activate hepatic NRF2 signaling in after one-week of commencing HFD feeding. Thus, in the current study, WA was able to modulate NRF2 signaling in a context-dependent manner.

NRF2 activation could improve glucose tolerance, suppress NASH and liver fibrosis, and attenuate liver cirrhosis (Wu et al., 2014; Sharma et al., 2018). This suggest that NRF2 could be

an efficient target for anti-NASH therapy, consistent with the report that pharmacological activation of NRF2 by the potent NRF2 activator TBE-31 is able to ameliorate experimental NASH (Sharma et al., 2018). Multiple mechanisms are involved in the modulation of NRF2 signaling via interfering with kelch like ECH associated protein 1-NRF2 interaction or other posttranscriptionally and/or posttranslationally-modulated mechanisms, such as ERAD-associated E3 ubiquitin-protein ligase HRD1, glycogen synthase kinase 3 and β-transducin repeat-containing protein (Chowdhry et al., 2013; Wu et al., 2014; Hayes et al., 2015). Among these known NRF2-modulating mechanisms, WA was demonstrated to be an inducer of NRF2 signaling both *in vitro* and *in vivo*, and this effect is partially kelch like ECH associated protein 1-independent and in part dependent on the glycogen synthase kinase 3 -associated modulation pathway as in the acetaminophen-induced acute liver injury model in mice (Palliyaguru et al., 2016). In the present study, the mechanisms by which WA attenuates NASH may be dependent on its effect on NRF2 signaling or other pathways such as NLRP3. This requires further experimentation using NRF2 and NLRP3 knockout mice that are beyond the scope of the current study.

In summary, by evaluating various NASH pathological parameters in serum and livers in two well-defined NASH mouse models (MCD-induced NASH model and HFD-induced NASH model in wide-type mice), WA exhibits both the preventive and therapeutic effects in improving NASH. WA also therapeutically decreases HFD-induced NASH in leptin-deficient ob/ob mice. The anti-NASH effect of WA is accompanied by lower hepatic oxidative stress, ER stress, and ceramide accumulation in serum. These data suggest that WA has potent anti-NASH effects at least independent of its anti-obesity effect as revealed in the non-obese MCD-induced NASH model and is independent of its leptin-sensitizing effect as found in a HFD-fed leptin-deficient ob/ob mouse NASH model. While further studies to determine the exact mechanisms by which

WA decreases NASH are still needed, these findings suggest that the herbal medicine-derived compound WA may be a therapeutic option for treating NASH particularly that featured with ceramide accumulation and would help repurpose the ancient drug WA with its novel application in treating NASH.

ACKNOWLEDGMENTS

We thank Linda G. Byrd submission and approval of the animal protocols, John Buckley, Linda G. Byrd, Ping Wang, and Yangliu Xia for help with animal experiments, and Chad N. Brocker, Jie Zhao, Cen Xie for expert advice.

AUTHOR CONTRIBUTIONS

Participated in research design: Yan, Patel, Gonzalez

Conducted experiments: Patel, Yan, Kim, Dias, Krausz

Performed data analysis: Patel, Yan, Dias

Wrote or contributed to the writing of the manuscript: Yan, Patel, Gonzalez, Kimura

GRANTS

This research was supported by the National Cancer Institute Intramural Research Program, Center for Cancer Research, National Institutes of Health; H.B.D. was supported by a fellowship from the CAPES Foundation, Ministry of Education of Brazil, Brasilia.

DISCLOSURES

No conflicts of interest, financial or otherwise, are declared by the authors.

REFERENCES

Bikman BT and Summers SA (2011) Ceramides as modulators of cellular and whole-body metabolism. *J Clin Invest* **121**:4222-4230.

Cassidy S and Syed BA (2016) Nonalcoholic steatohepatitis (NASH) drugs market. *Nat Rev Drug Discov* **15**:745-746.

Chaurasia B and Summers SA (2015) Ceramides - lipotoxic inducers of metabolic disorders. *Trends Endocrinol Metab* **26**:538-550.

Chowdhry S, Zhang Y, McMahon M, Sutherland C, Cuadrado A and Hayes JD (2013) Nrf2 is controlled by two distinct beta-TrCP recognition motifs in its Neh6 domain, one of which can be modulated by GSK-3 activity. *Oncogene* **32**:3765-3781.

Ding ZM, Xiao Y, Wu X, Zou H, Yang S, Shen Y, Xu J, Workman HC, Usborne AL and Hua H (2018) Progression and regression of hepatic lesions in a mouse model of NASH induced by dietary intervention and Its implications in pharmacotherapy. *Front Pharmacol* **9**:410.

Dubey S, Yoon H, Cohen MS, Nagarkatti P, Nagarkatti M and Karan D (2018) Withaferin A associated differential regulation of inflammatory cytokines. *Front Immunol* **9**:195.

Estes C, Razavi H, Loomba R, Younossi Z and Sanyal AJ (2018) Modeling the epidemic of nonalcoholic fatty liver disease demonstrates an exponential increase in burden of disease. *Hepatology* **67**:123-133.

Farrell GC and Larter CZ (2006) Nonalcoholic fatty liver disease: from steatosis to cirrhosis. *Hepatology* **43**:S99-S112.

Flemming JA, Kim WR, Brosgart CL and Terrault NA (2017) Reduction in liver transplant wait-listing in the era of direct-acting antiviral therapy. *Hepatology* **65**:804-812.

Friedman SL, Neuschwander-Tetri BA, Rinella M and Sanyal AJ (2018) Mechanisms of NAFLD development and therapeutic strategies. *Nat Med* **24**:908-922.

Griffett K, Welch RD, Flaveny CA, Kolar GR, Neuschwander-Tetri BA and Burris TP (2015) The LXR inverse agonist SR9238 suppresses fibrosis in a model of non-alcoholic steatohepatitis. *Mol Metab* **4**:353-357.

Hayes JD, Chowdhry S, Dinkova-Kostova AT and Sutherland C (2015) Dual regulation of transcription factor Nrf2 by Keap1 and by the combined actions of beta-TrCP and GSK-3. *Biochem Soc Trans* **43**:611-620.

Hebbard L and George J (2011) Animal models of nonalcoholic fatty liver disease. *Nat Rev Gastroenterol Hepatol* **8**:35-44.

Heyninck K, Sabbe L, Chirumamilla CS, Szarc Vel Szic K, Vander Veken P, Lemmens KJA, Lahtela-Kakkonen M, Naulaerts S, Op de Beeck K, Laukens K, Van Camp G, Weseler AR, Bast A, Haenen G, Haegeman G and Vanden Berghe W (2016) Withaferin A induces heme oxygenase (HO-1) expression in endothelial cells via activation of the Keap1/Nrf2 pathway. *Biochem Pharmacol* **109**:48-61.

Honda Y, Imajo K, Kato T, Kessoku T, Ogawa Y, Tomeno W, Kato S, Mawatari H, Fujita K, Yoneda M, Saito S and Nakajima A (2016) The selective SGLT2 inhibitor ipragliflozin has a therapeutic effect on nonalcoholic steatohepatitis in mice. *Plos One* **11**:e0146337.

Jadeja RN, Urrunaga NH, Dash S, Khurana S and Saxena NK (2015) Withaferin-A reduces acetaminophen-induced liver injury in mice. *Biochem Pharmacol* **97**:122-132.

Javor ED, Cochran EK, Musso C, Young JR, Depaoli AM and Gorden P (2005) Long-term efficacy of leptin replacement in patients with generalized lipodystrophy. *Diabetes* **54**:1994-2002.

Jiang C, Xie C, Li F, Zhang L, Nichols RG, Krausz KW, Cai J, Qi Y, Fang ZZ, Takahashi S, Tanaka N, Desai D, Amin SG, Albert I, Patterson AD and Gonzalez FJ (2015) Intestinal farnesoid X receptor signaling promotes nonalcoholic fatty liver disease. *J Clin Invest* **125**:386-402.

Kasumov T, Li L, Li M, Gulshan K, Kirwan JP, Liu XL, Previs S, Willard B, Smith JD and McCullough A (2015) Ceramide as a mediator of non-alcoholic fatty liver disease and associated atherosclerosis. *Plos One* **10**:e01269.

Kim JE, Lee JY, Kang MJ, Jeong YJ, Choi JA, Oh SM, Lee KB and Park JH (2015) Withaferin A Inhibits helicobacter pylori-induced production of IL-1beta in dendritic cells by regulating NF-kappaB and NLRP3 inflammasome activation. *Immune Netw* **15**:269-277.

Kurek K, Piotrowska DM, Wiesiolek-Kurek P, Lukaszuk B, Chabowski A, Gorski J and Zendzian-Piotrowska M (2014) Inhibition of ceramide de novo synthesis reduces liver lipid accumulation in rats with nonalcoholic fatty liver disease. *Liver Int* **34**:1074-1083.

Lee IC and Choi BY (2016) Withaferin-A-a natural anticancer agent with pleitropic mechanisms of action. *Int J Mol Sci* **17**.

Lee J, Liu JL, Feng XD, Hernandez MAS, Mucka P, Ibi D, Choi JW and Ozcan U (2016) Withaferin A is a leptin sensitizer with strong antidiabetic properties in mice. *Nat Med* **22**:1023-1032.

Longato L, Tong M, Wands JR and de la Monte SM (2012) High fat diet induced hepatic steatosis and insulin resistance: Role of dysregulated ceramide metabolism. *Hepatol Res* **42**:412-427.

Michelotti GA, Machado MV and Diehl AM (2013) NAFLD, NASH and liver cancer. *Nat Rev Gastroenterol Hepatol*. **10**:656-665.

Oseini AM and Sanyal AJ (2017) Therapies in non-alcoholic steatohepatitis (NASH). *Liver Int* **37 Suppl 1**:97-103.

Pagadala M, Kasumov T, McCullough AJ, Zein NN and Kirwan JP (2012) Role of ceramides in nonalcoholic fatty liver disease. *Trends Endocrinol Metab* **23**:365-371.

Palliyaguru DL, Chartoumpekis DV, Wakabayashi N, Skoko JJ, Yagishita Y, Singh SV and Kensler TW (2016) Withaferin A induces Nrf2-dependent protection against liver injury: Role of Keap1-independent mechanisms. *Free Radic Biol Med* **101**:116-128.

Polyzos SA, Kountouras J and Mantzoros CS (2015) Leptin in nonalcoholic fatty liver disease: a narrative review. *Metabolism* **64**:60-78.

Scott N, McBryde E, Vickerman P, Martin NK, Stone J, Drummer H and Hellard M (2015) The role of a hepatitis C virus vaccine: modelling the benefits alongside direct-acting antiviral treatments. *BMC Med* **13**:198.

Sharma RS, Harrison DJ, Kisielewski D, Cassidy DM, McNeilly AD, Gallagher JR, Walsh SV, Honda T, McCrimmon RJ, Dinkova-Kostova AT, Ashford MLJ, Dillon JF and Hayes JD (2018) Experimental Nonalcoholic Steatohepatitis and Liver Fibrosis Are Ameliorated by Pharmacologic Activation of Nrf2 (NF-E2 p45-Related Factor 2). *Cell Mol Gastroenter* **5**:367-398.

Thaiparambil JT, Bender L, Ganesh T, Kline E, Patel P, Liu Y, Tighiouart M, Vertino PM, Harvey RD, Garcia A and Marcus AI (2011) Withaferin A inhibits breast cancer invasion and metastasis at sub-cytotoxic doses by inducing vimentin disassembly and serine 56 phosphorylation. *Int J Cancer* **129**:2744-2755.

Vanden Berghe W, Sabbe L, Kaileh M, Haegeman G and Heyninck K (2012) Molecular insight in the multifunctional activities of Withaferin A. *Biochem Pharmacol* **84**:1282-1291.

Vedi M and Sabina EP (2016) Assessment of hepatoprotective and nephroprotective potential of withaferin A on bromobenzene-induced injury in Swiss albino mice: possible involvement of mitochondrial dysfunction and inflammation. *Cell Biol Toxicol* **32**:373-390.

Wong RJ, Aguilar M, Cheung R, Perumpail RB, Harrison SA, Younossi ZM and Ahmed A (2015) Nonalcoholic steatohepatitis Is the second leading etiology of liver disease among adults awaiting liver transplantation in the United States. *Gastroenterology* **148**:547-555.

Wong RJ, Cheung R and Ahmed A (2014) Nonalcoholic steatohepatitis is the most rapidly growing indication for liver transplantation in patients with hepatocellular carcinoma in the U. S. *Hepatology* **59**:2188-2195.

Wu T, Zhao F, Gao B, Tan C, Yagishita N, Nakajima T, Wong PK, Chapman E, Fang D and Zhang DD (2014) Hrd1 suppresses Nrf2-mediated cellular protection during liver cirrhosis. *Genes Dev* **28**:708-722.

Xie C, Yagai T, Luo Y, Liang X, Chen T, Wang Q, Sun D, Zhao J, Ramakrishnan SK, Sun L, Jiang C, Xue X, Tian Y, Krausz KW, Patterson AD, Shah YM, Wu Y, Jiang C and Gonzalez FJ (2017) Activation of intestinal hypoxia-inducible factor 2alpha during obesity contributes to hepatic steatosis. *Nat Med* **23**:1298-1308.

Yan TT, Wang H, Cao LJ, Wang Q, Takahashi S, Yagai T, Li GL, Krausz KW, Wang GJ, Gonzalez FJ and Hao HP (2018) Glycyrrhizin alleviates nonalcoholic steatohepatitis via modulating bile acids and meta-inflammation. *Drug Metab Dispos* **46**:1310-1319.

Figure Legends

Fig. 1: Effect of WA in body weight, liver weight, liver index and liver histology in MCS diet-fed mice. (A) Experiment scheme for testing the preventive effects of WA in the MCD-induced liver injury model; **(B)** Effect of WA on body weight; **(C)** Effect of WA on liver weight; **(D)**, Effect of WA on liver index; **(E)**, Effect of WA on H&E staining of MCS diet-fed mouse livers. Scale bar size, 100 μm. Data were presented as means ± SD. MCS, mice fed the MCS diet and treated with vehicle; MCS+WA5, mice fed the MCS diet and treated with 5 mg/kg of WA only; MCD, mice fed the MCD diet and treated with vehicle; MCD+WA1, mice fed the MCD diet and treated with 1 mg/kg of WA; MCD+WA2.5, mice fed the MCD diet and treated with 2.5 mg/kg of WA; MCD+WA5, mice fed the MCD diet and treated with 5 mg/kg of WA. n=5 mice per group. Statistical differences were determined by the two-tailed t test between two groups or by one-way ANOVA among multiple MCD diet-fed groups. $^{###}P<0.005$ when compared with MCS group; * $P<0.05$ and ** $P<0.01$ when compared with the MCD group.

Fig. 2: WA dose-dependently alleviated MCD diet-induced liver injury. (A and B) Analysis of serum ALT (**A**) and AST levels (**B**). **(C and D)** Analysis of liver TC (**C**) and TG (**D**) levels. **(E and F)** Analysis of serum TC (**E**) and TG levels (**F**). **(G)** Analysis of hepatic pro-inflammatory cytokines mRNA levels. **(H)** H & E staining of livers from MCD diet-fed mice treated with vehicle or 5 mg/kg of WA. **(I)** Oil Red O staining of livers from MCD diet-fed mice treated with vehicle or 5 mg/kg of WA. Scale bar, 100 μm. Data were presented as means ± SD. Group descriptions for the MCS, MCS+WA5, MCD, MCD+WA1, MCD+WA2.5, MCD+WA5 groups were the same as described in the legend to Fig. 1. n=5 mice per group. $^{#}P<0.05$, $^{##}P<0.01$ and $^{###}P<0.005$ when compared with the MCS group; *$P<0.05$, **$P<0.01$, ***$P<0.005$ when compared with the MCD

group. Statistical differences were determined by the two-tailed t test or one-way ANOVA. *Tnfa*, tumor necrosis factor alpha; *Il1b*, interleukin 1b; *Il6*, interleukin 6.

Fig. 3: WA alleviated MCD diet-induced liver injury independent of body weight change. **(A)** Experiment scheme for testing the therapeutic effect of WA in MCD diet-induced NASH model; **(B)** Body weights; **(C)** liver weights; **(D)** Liver indexes calculated as the ratio of liver weight to body weight; **(E)** serum ALT levels; **(F)** serum AST levels. Data were presented as means ± SD. Group descriptions for MCS, MCD, and MCD+WA5 were same as described in the legend to Fig. 1. n=5 mice per group. Data were presented as means ± SD. Statistical differences were determined by the two-tailed t test between two groups. *P<0.05 and ***P<0.005 compared with MCD group.

Fig. 4: WA therapeutically improved MCD diet-induced NASH. **(A)** Experiment scheme for testing the therapeutic effect of WA in the MCD-induced NASH model. **(B)** Effect of 5 mg/kg WA on body weight. **(C)** Effect of 5 mg/kg WA on liver weight. **(D)** Effect of 5 mg/kg WA on liver indexes. **(E and F)** Analysis of serum ALT (**E**) and AST (**F**) levels in LFD-fed mice and HFD-fed mice treated with control vehicle or WA. **(G and H)** Histology analysis of hepatic steatosis by Oil Red O staining (**G**) and H & E staining (**H**). Scale bar, 100 μm. Data were presented as means ± SD. Descriptions for the MCS, MCS+WA5, MCD, MCD+WA5 groups were same as described in the legend to Fig. 1. n=5 mice per group. $^{\#}$P<0.05, $^{\#\#}$P<0.01 and $^{\#\#\#}$P<0.005 when compared with MCS group; *P<0.05 when compared with MCD group. Statistical differences were determined by the two-tailed t test or one-way ANOVA.

Fig. 5: WA improved HFD-induced liver injury. (A) Experiment scheme of the time-course dosing regimen. **(B and C)** Body weights of HFD-fed mice (**B**) and LFD-fed mice (**C**) treated with vehicle or WA. **(D and E)** Liver weights (**D**) and liver indexes calculated by liver weight/body weight ratio (E). **(F and G)** Analysis of serum ALT (**F**) and AST levels (**G**). Data were presented as means ± SD. LV, mice fed the LFD and treated with vehicle (V); L+4W WA, mice fed LFD and treated with WA for the last 4 weeks. L+8W WA, mice fed the LFD and treated with WA for the last 8 weeks; L+12W WA, mice fed the LFD and treated with WA for the last 12 weeks; NV, mice fed the HFD-induced NASH diet (N) and treated with vehicle (V); N+4W WA, mice fed the HFD-induced NASH diet (N) and treated with WA for the last four weeks; N+8W WA, mice fed the HFD-induced NASH diet (N) and treated with WA for the last 8 weeks; N+12W WA, mice fed the HFD-induced NASH diet (N) and treated with WA for the last 12 weeks. n=5 mice for the LFD-fed groups and n=7-10 for HFD-fed mice. $^{\#\#}P<0.01$ and $^{\#\#\#}P<0.005$ compared with the LFD group; $*P<0.05$ and $***P<0.005$ compared with HFD group. Statistical differences were determined by the two-tailed t test or one-way ANOVA.

Fig. 6: WA improved serum and liver biochemical parameters in a time-dependent manner. (A and B) Analysis of liver TG levels (**A**) and TC levels (**B**). **(C and D)** Analysis of serum TG (**C**) and TC (**D**) levels. **(E and F)** Analysis of liver NEFAs levels (E) and serum NEFAs levels (**F**). Data were presented as means ± SD. Groups for the LV, NV, N+4W WA, N+8W WA, and N+12W WA groups were same as described in the legend to Fig. 5. n=5 mice for the LFD group and n=7-10 for the other three HFD-fed groups. $^{\#\#}P<0.01$ and $^{\#\#\#}P<0.005$ compared with LFD group; $**P<0.01$ and $***P<0.005$ compared with the HFD group. Statistical differences were determined by the two-tailed t test or one-way ANOVA.

JPET Fast Forward. Published on August 16, 2019 as DOI: 10.1124/jpet.119.256792
This article has not been copyedited and formatted. The final version may differ from this version.

Fig. 7: WA improved HFD-induced hepatic steatosis and inflammation. (A and B) Representative histology pictures of H & E staining (**A**) and Oil Red O staining (**B**). Scale bar, 100 μm. **(C-E)** Effect of WA on HFD-induced liver *Tnfa*, *Il1b*, and *Il6* mRNA levels. **(F-G)** Effect of WA on HFD-induced hepatic ER stress signaling markers, *Hspa5* and *Didt3,* mRNAs levels. **(H-J)** Effect of WA on HFD-induced *Srebp1c*, *Fas*, and *Scd1* mRNAs levels. Data were presented as means ± SD. Descriptions for the LV, NV, N+4W WA, N+8W WA, and N+12W WA were same as described in the legend to Fig. 5. n=5 mice for the LFD group and n=7-10 for the other three HFD-fed groups. ###P<0.005 compared with LFD group; *P<0.05, **P<0.01 and ***P<0.005 compared with the HFD group. Statistical differences were determined by the two-tailed t test or one-way ANOVA.

Fig. 8: WA improved HFD-induced hepatic fibrosis. (A) Representative hepatic picrosirius red staining for both LFD-fed livers and HFD-fed livers. Scale bar, 100 μm. **(B)** Statistical quantitation analysis of picrosirius red staining for liver collagen. **(C-F)** Analysis of *Timp2*, *Col1a1*, *Mmp2*, and *Acta2* mRNAs. Data were presented as means ± SD. Descriptions for the LV, NV, N+4W WA, N+8W WA, and N+12W WA groups were same as described in the legend to Fig. 5. n=5 mice for LFD group and n=7-10 for the other three HFD-fed groups. ###P<0.005 when compared with the LFD group; *P<0.05, **P<0.01, while ***P<0.005 when compared with the HFD group. Statistical differences were determined by the two-tailed t test or one-way ANOVA.

Fig. 9: WA rescued HFD-induced ceramides accumulation and oxidative stress. (A-G) Quantitation of serum ceramide concentrations for C16 (**A**), C18 (**B**), C20 (**C**), C22 (**D**), C24 (E),

C18:1 (**F**) and C24:1 (**G**). **(H-J)** Analysis of hepatic superoxide dismutase levels (H), glutathione levels (**I**) and peroxide levels. (**J**) Data were presented as means ± SD. Descriptions for the LV, NV, N+4W WA, N+8W WA, and N+12W WA groups were same as described in the legend to Fig. 5. n=5 mice for the LFD-fed groups and n=7-10 for the HFD-fed groups. ###P<0.005 compared with the LFD group; *P<0.05, ** P<0.01 and *** P<0.005 compared with HFD group. Statistical differences were determined by the two-tailed t test or one-way ANOVA.

Fig. 10: WA treatment reduced ceramides biosynthesis and catabolism in WA treated HFD-fed C57bl/6N mice and ER-stress markers in a time dependent manner. (A-M) Ceramides biosynthesis and catabolism markers analysis of *Sptlc1* **(A)**, *Sptlc2* **(B)**, *Smpd1* **(C)**, *Smpd2* **(D)**, *Smpd3* **(E)**, *Smpd4* **(F)**, *Acer2* **(G)**, *Acer3* **(H)**, *Sgms1* **(I)**, *Sgms2* **(J)**, *Cers2* **(K)**, *Cers4* **(L)** and *Cers6* **(M)** mRNA levels. Descriptions for the LV, NV, N+4W WA, N+8W WA, and N+12W WA were same as described in the legend to Fig. 5. n=5 mice for the LFD group and n=7-10 for the other three HFD-fed groups. ###P<0.005 compared with LFD group; *P<0.05, **P<0.01, and *** P<0.005 compared with the HFD group. Statistical differences were determined by the two-tailed t test or one-way ANOVA.

Fig. 11: WA improved HFD-induced liver injury in ob/ob mice and liver histology. (A) Experimental scheme for testing the therapeutic effect of WA in the HFD diet-induced NASH model. **(B)** Body weights. **(C and D)** liver weights **(C)** and liver indexes calculated by liver weight/body weight ratios **(D)**. **(E and F)** Analysis of serum ALT (**E**) and AST levels (**F**). **(G and H)** Representative histology pictures of H & E staining (**G**) and Oil Red O staining (**H**) for HFD and WA treated HFD livers. Scale bar, 100 μm. (**I**) Effect of WA on HFD-induced liver *Il1b*, *Il6,*

Tnfa, *Srebp1c*, *Fas*, and *Scd1* mRNAs levels. Data were presented as means ± SD. NV, mice fed the HFD-induced NASH diet (N) and treated with vehicle (V) for 12 weeks; N+ WA5, mice fed the HFD diet and treated with 5 mg/kg of WA mice fed the HFD-induced NASH diet (N) and treated with WA for the last four weeks; n=5 mice for the HFD-fed vehicle groups and n=8 for WA treated HFD-fed ob/ob mice. *P<0.05, **P<0.01, and ***P<0.005 compared with HFD group. Statistical differences were determined by the two-tailed t test.

Fig. 12: WA treatment improved serum and liver biochemical parameters, reduces HFD-induced hepatic fibrosis, and mRNAs associated with ER-stress and ceramides biosynthesis and catabolism in WA-treated HFD-fed ob/ob mice. (A-F) Analysis of liver TG levels (**A**), TC levels (**B**); NEFAs levels **(C);** analysis of serum TG (**D**) serum TC (**D**) levels and serum NEFAs levels (**F**). **(G)** Hepatic fibrosis markers analysis of *Timp2*, *Col1a1*, *Mmp2*, and *Acta2* mRNAs levels. **(H)** Representative hepatic picrosirius red staining for HFD and WA treated HFD livers, Scale bar 100 μm. **(I)** Hepatic endoplasmic reticulum stress signaling markers analysis of *Hspa5* and *Didt3* mRNA levels **(J)** *Sptlc1*, *Sptlc2*, *Smpd2*, *Smpd3*, *Acer1*, *Acer2*, *Sgms1*, *Sgms2*, *Cers2*, *Cers4* and *Cers6* mRNA levels. Data were presented as means ± SD. NV, mice fed the HFD-induced NASH diet (N) and treated with vehicle (V) for 12 weeks; N+ WA5, mice fed the HFD diet and treated with 5 mg/kg of WA mice fed the HFD-induced NASH diet (N) and treated with WA for the last four weeks; n=5 mice for the HFD-fed vehicle groups and n=8 for WA treated HFD-fed ob/ob mice. *P<0.05, **P<0.01 and ***P<0.005 compared with HFD group. Statistical differences were determined by the two-tailed t test.

Fig. 13: Summary of major findings and proposed mechanism. In the current study, withaferin A (WA) was found to have both preventive and therapeutic effects in treating NASH as assessed by using two NASH models. MCD diet feeding, on the other hand, induced weight loss and thus was called the "Lean NASH" model, while the HFD-induced obesity was referred to as the "Obese NASH" model. HFD feeding induced oxidative stress and oxidative stress could contribute to the increase in serum ceramide accumulation that was known to promote the progression of NASH. In the HFD-induced obese NASH model, WA alleviated HFD-induced oxidative stress as revealed by the decreased H_2O_2 and increased glutathione and superoxide dismutase levels. WA also significantly alleviated HFD-induced ceramides accumulation in serum. However, other factors could also contribute to ceramide accumulation in the HFD-induced NASH model and how WA affects them still requires further study. Abbreviations used: MCD, methionine and choline deficient; HFD, high-fat diet; NASH, non-alcoholic steatohepatitis.

JPET Fast Forward. Published on August 16, 2019 as DOI: 10.1124/jpet.119.256792
This article has not been copyedited and formatted. The final version may differ from this version.

Figure 1

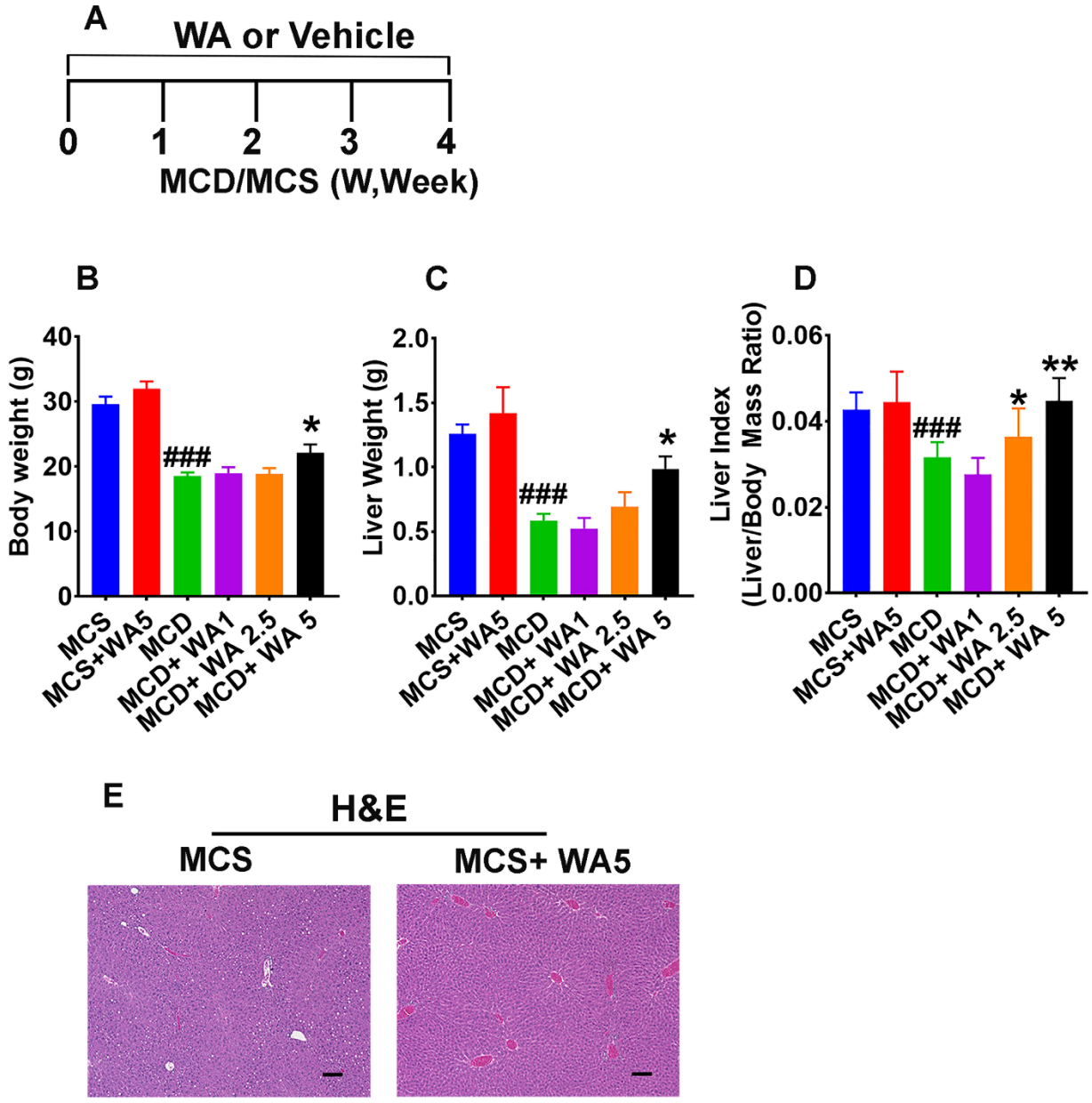

JPET Fast Forward. Published on August 16, 2019 as DOI: 10.1124/jpet.119.256792
This article has not been copyedited and formatted. The final version may differ from this version.

Figure 2

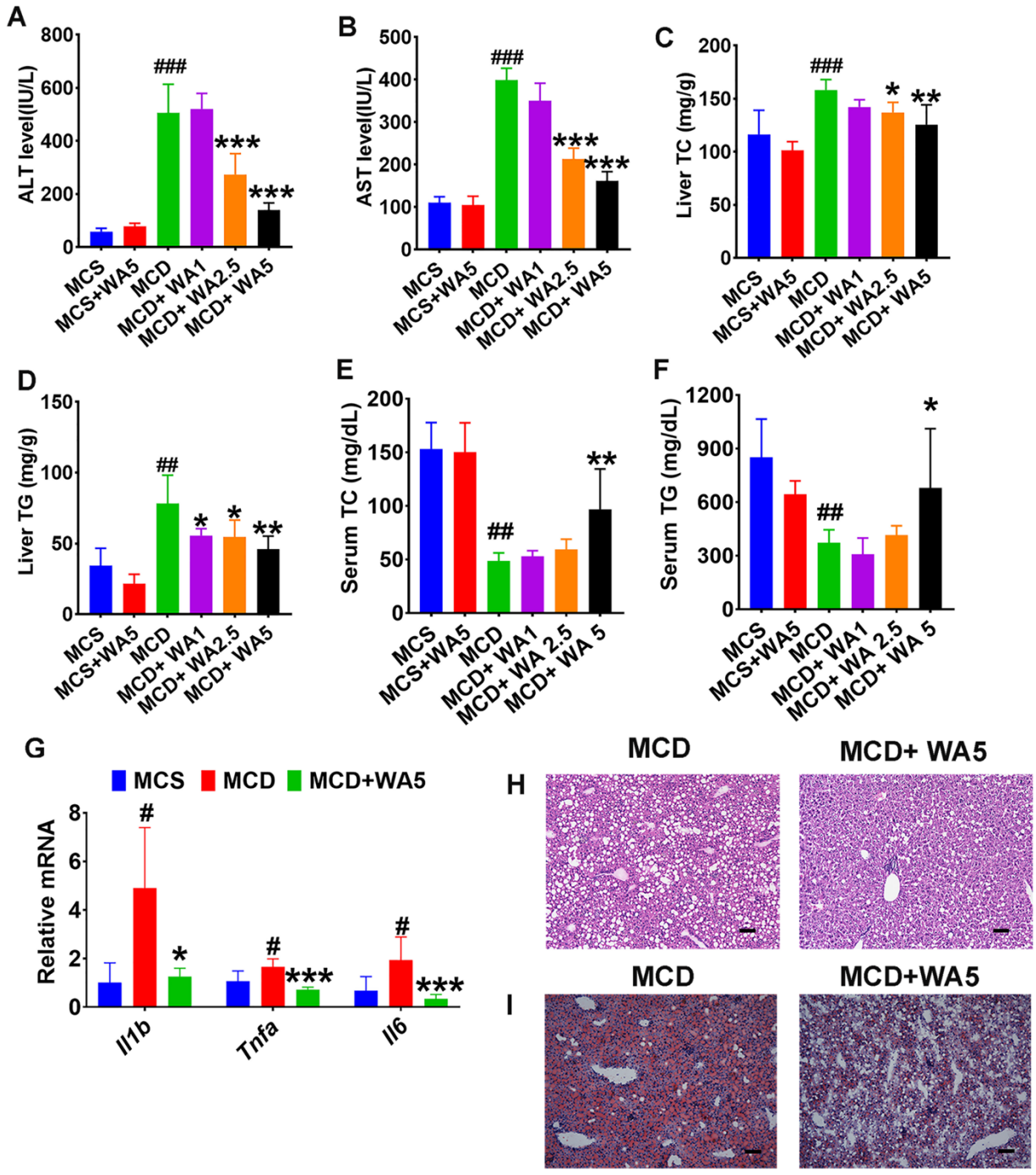

JPET Fast Forward. Published on August 16, 2019 as DOI: 10.1124/jpet.119.256792
This article has not been copyedited and formatted. The final version may differ from this version.

Figure 3

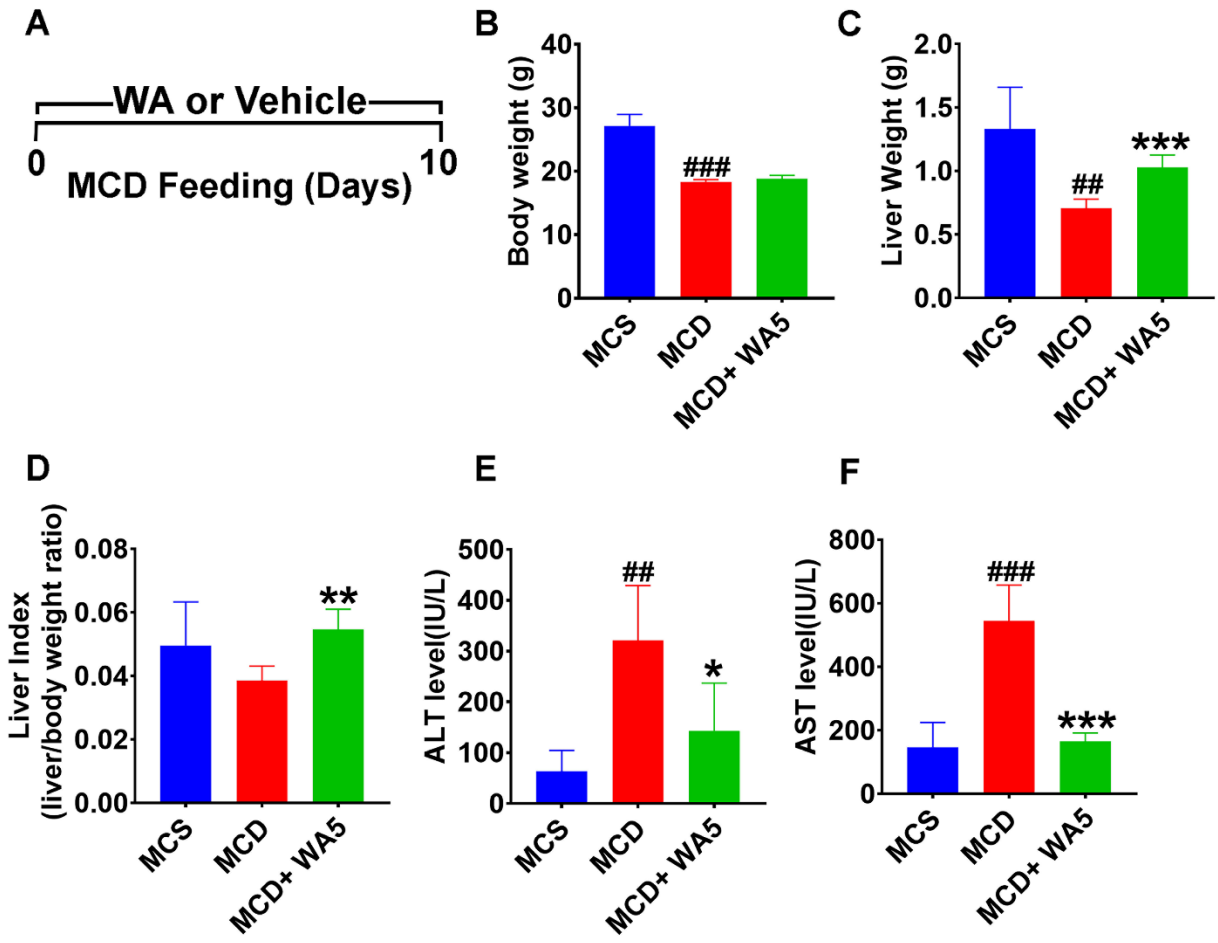

JPET Fast Forward. Published on August 16, 2019 as DOI: 10.1124/jpet.119.256792
This article has not been copyedited and formatted. The final version may differ from this version.

Figure 4

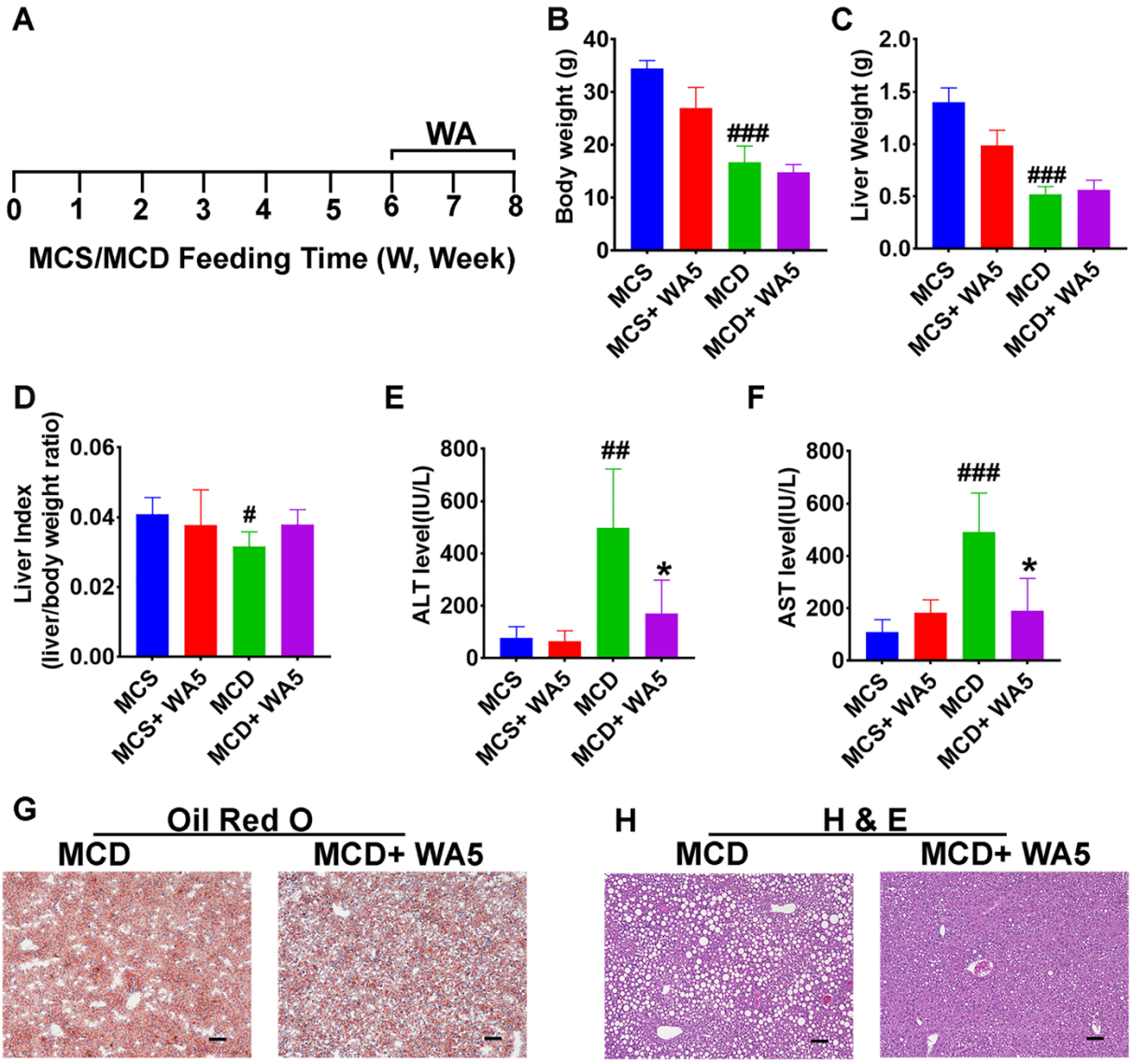

JPET Fast Forward. Published on August 16, 2019 as DOI: 10.1124/jpet.119.256792
This article has not been copyedited and formatted. The final version may differ from this version.

Figure 5

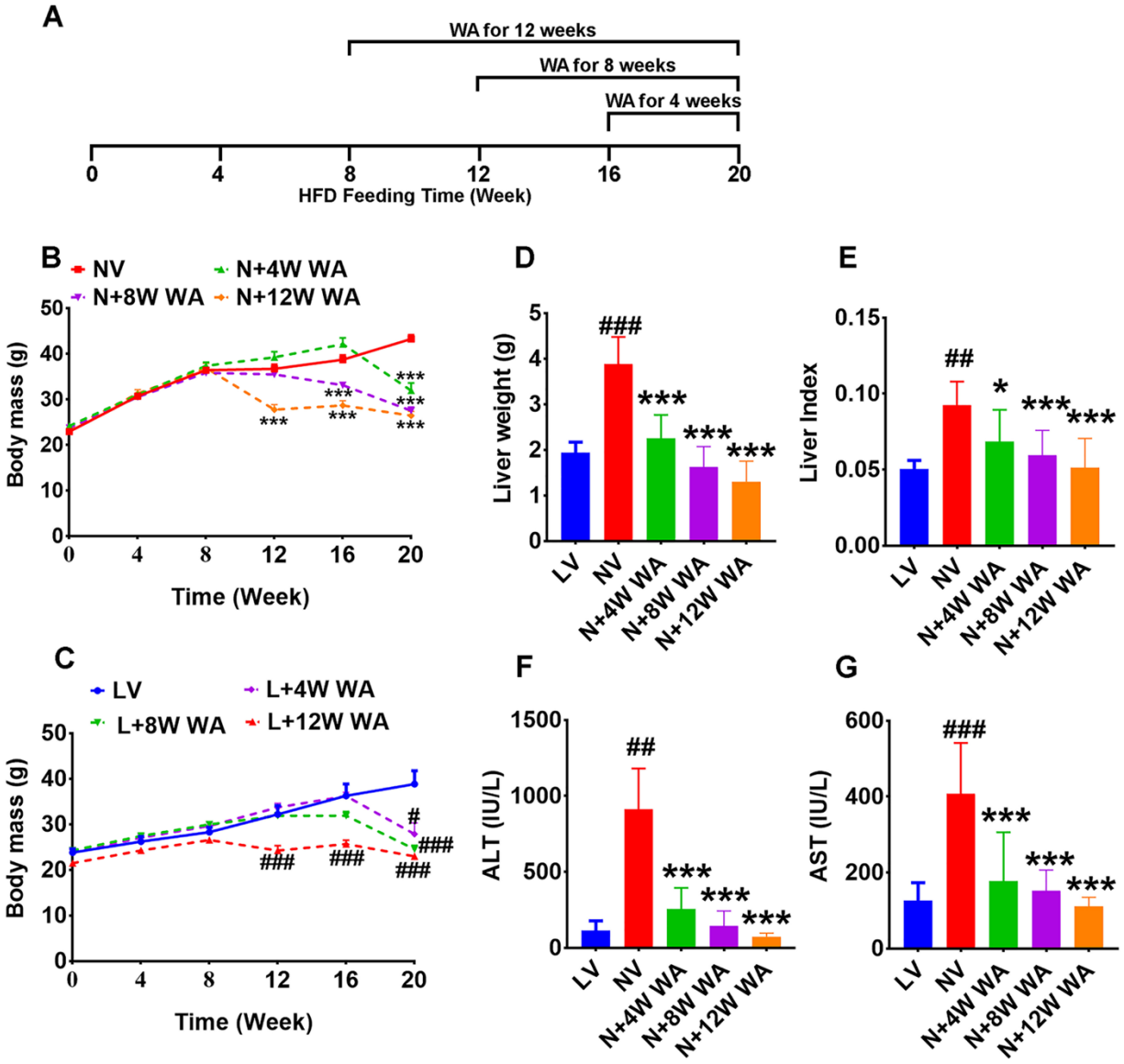

JPET Fast Forward. Published on August 16, 2019 as DOI: 10.1124/jpet.119.256792
This article has not been copyedited and formatted. The final version may differ from this version.

Figure 6

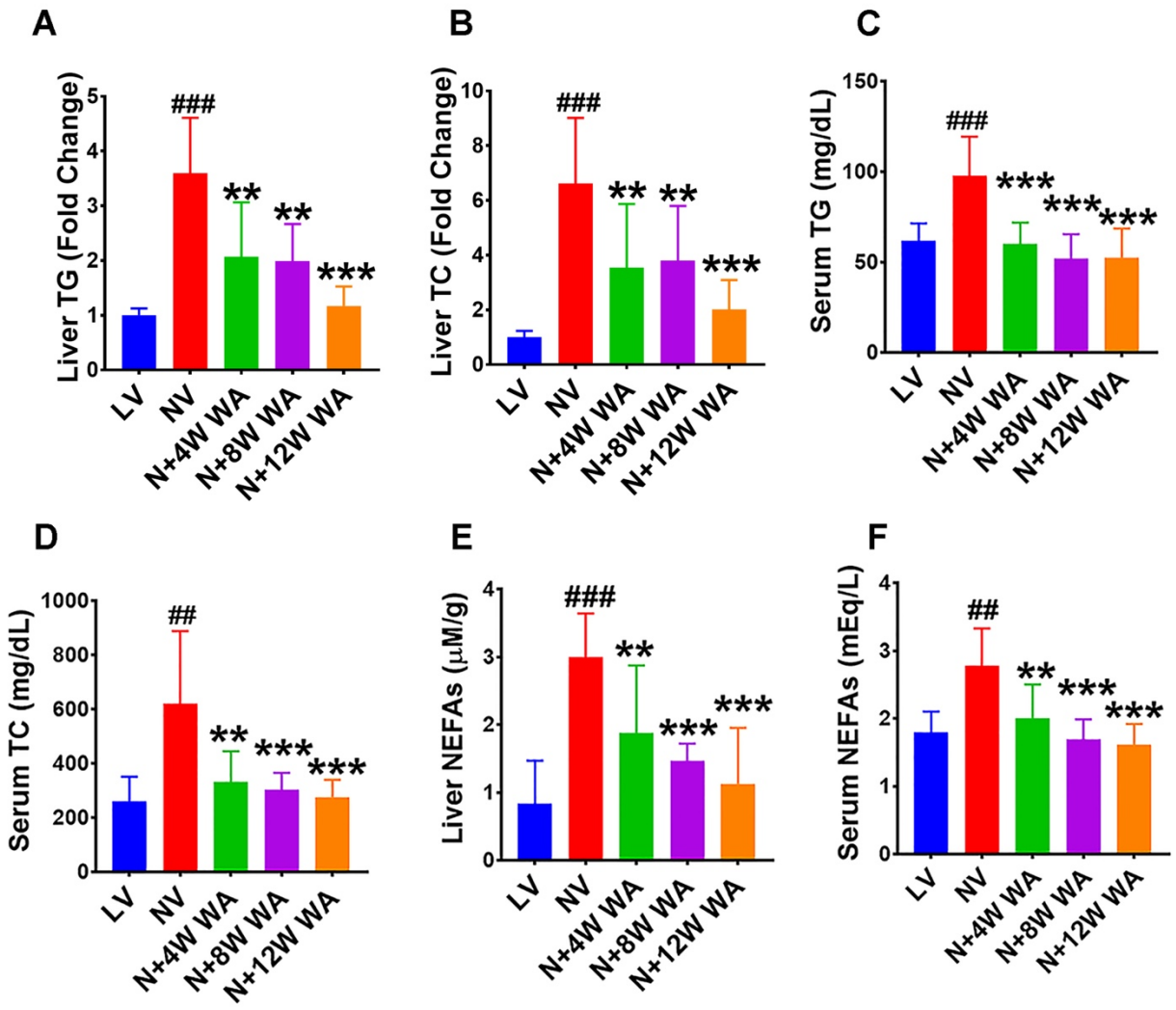

JPET Fast Forward. Published on August 16, 2019 as DOI: 10.1124/jpet.119.256792
This article has not been copyedited and formatted. The final version may differ from this version.

Figure 7

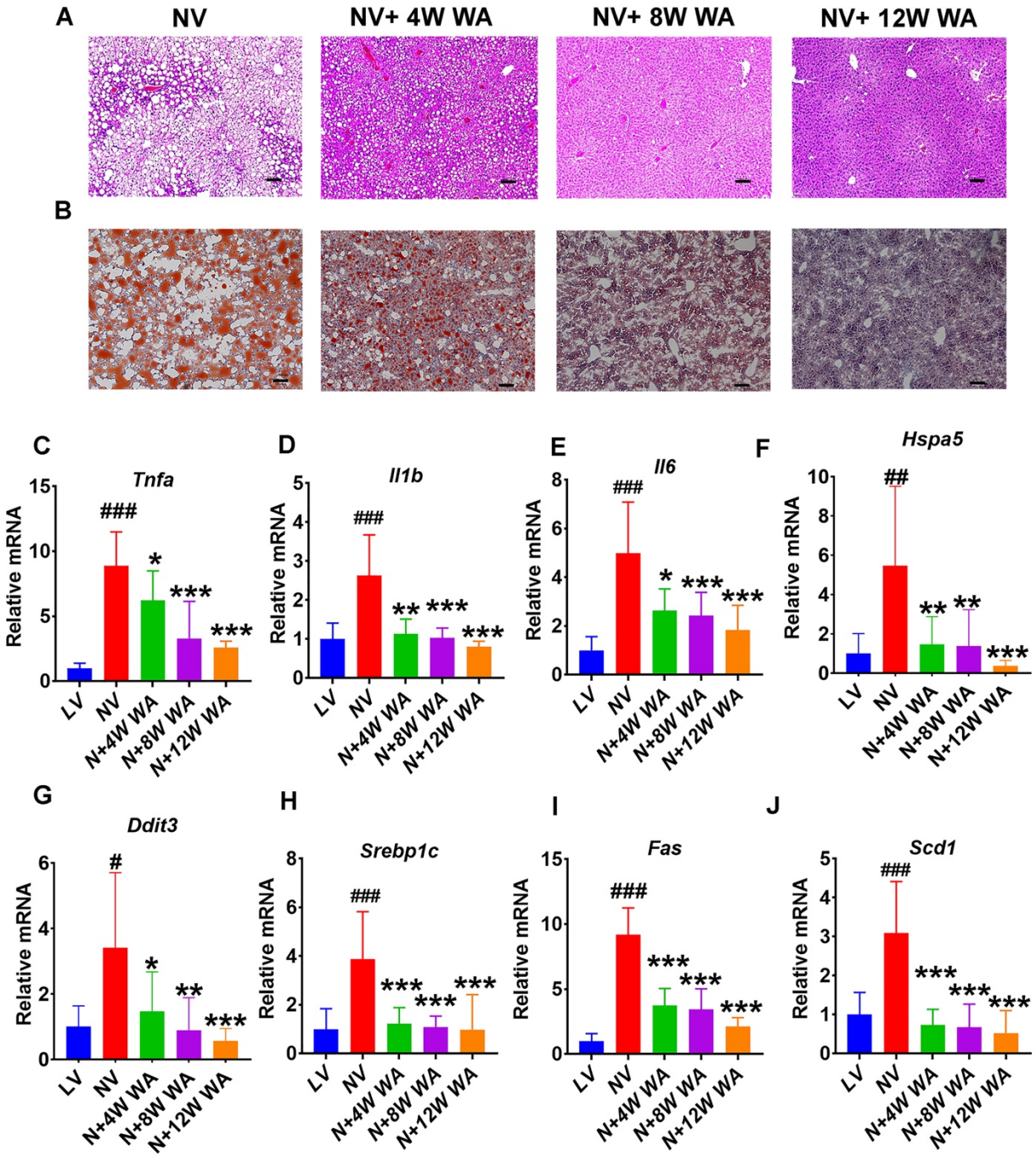

JPET Fast Forward. Published on August 16, 2019 as DOI: 10.1124/jpet.119.256792
This article has not been copyedited and formatted. The final version may differ from this version.

Figure 8

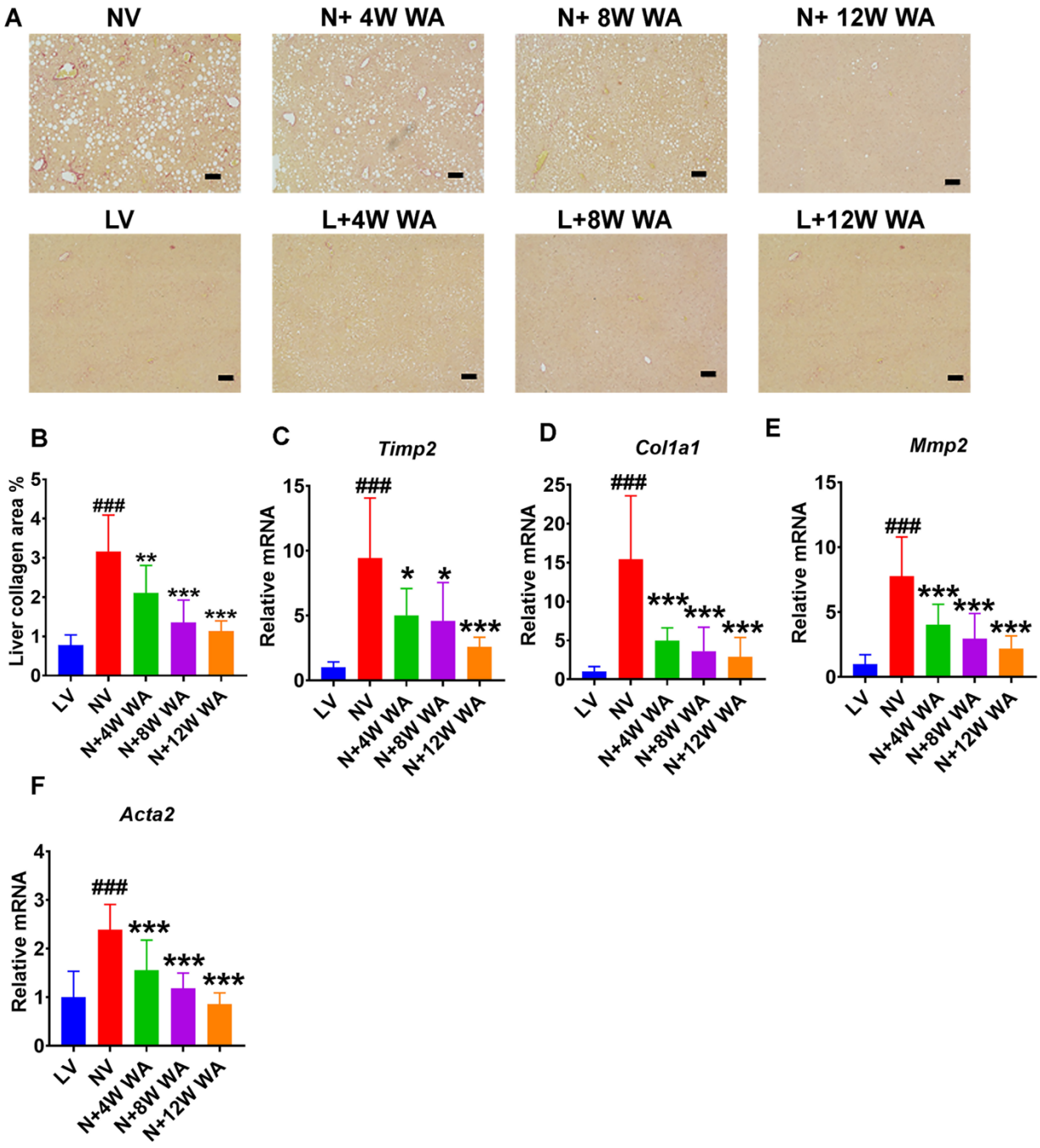

JPET Fast Forward. Published on August 16, 2019 as DOI: 10.1124/jpet.119.256792
This article has not been copyedited and formatted. The final version may differ from this version.

Figure 9

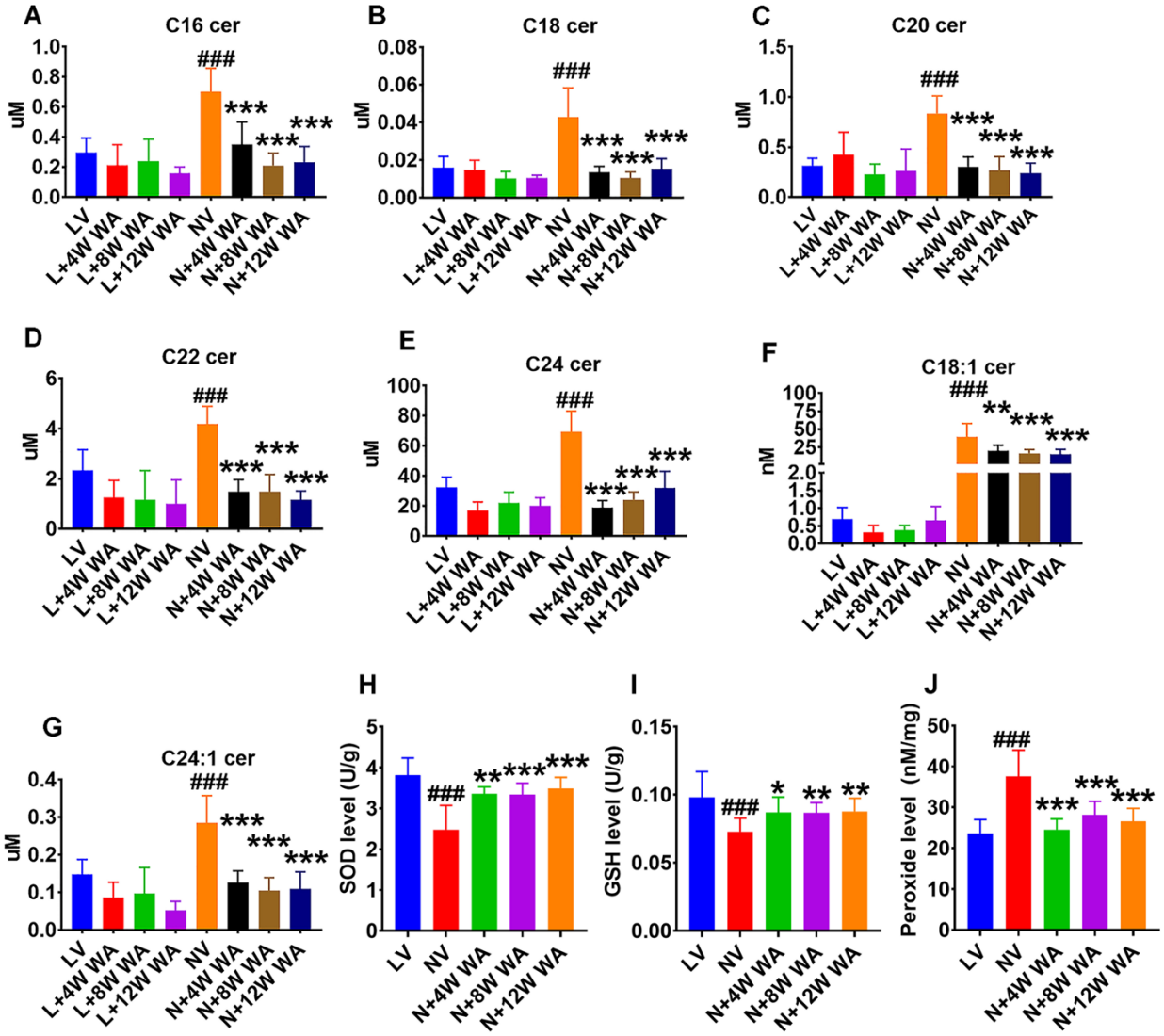

JPET Fast Forward. Published on August 16, 2019 as DOI: 10.1124/jpet.119.256792
This article has not been copyedited and formatted. The final version may differ from this version.

Figure 10

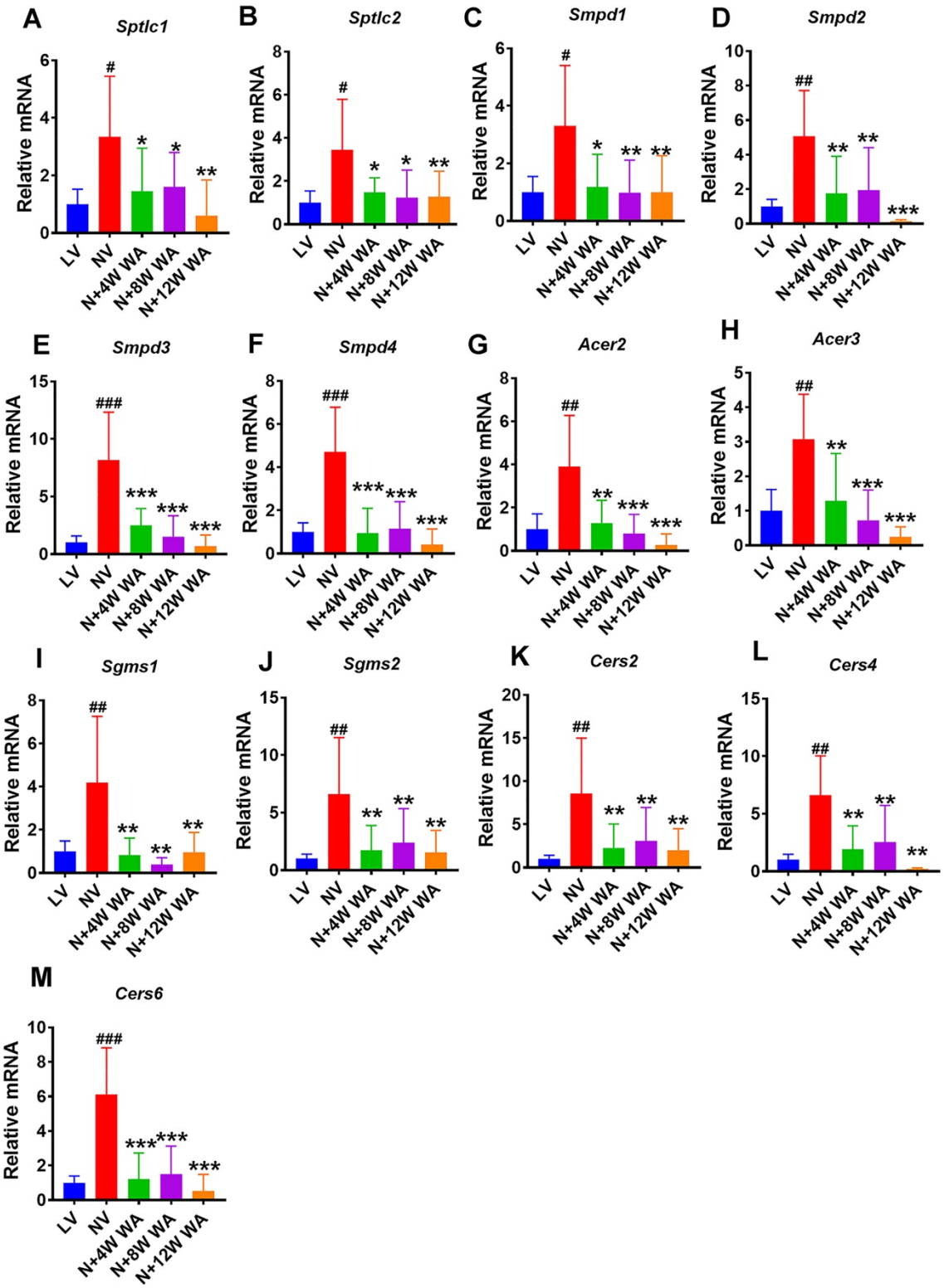

JPET Fast Forward. Published on August 16, 2019 as DOI: 10.1124/jpet.119.256792
This article has not been copyedited and formatted. The final version may differ from this version.

Figure 11

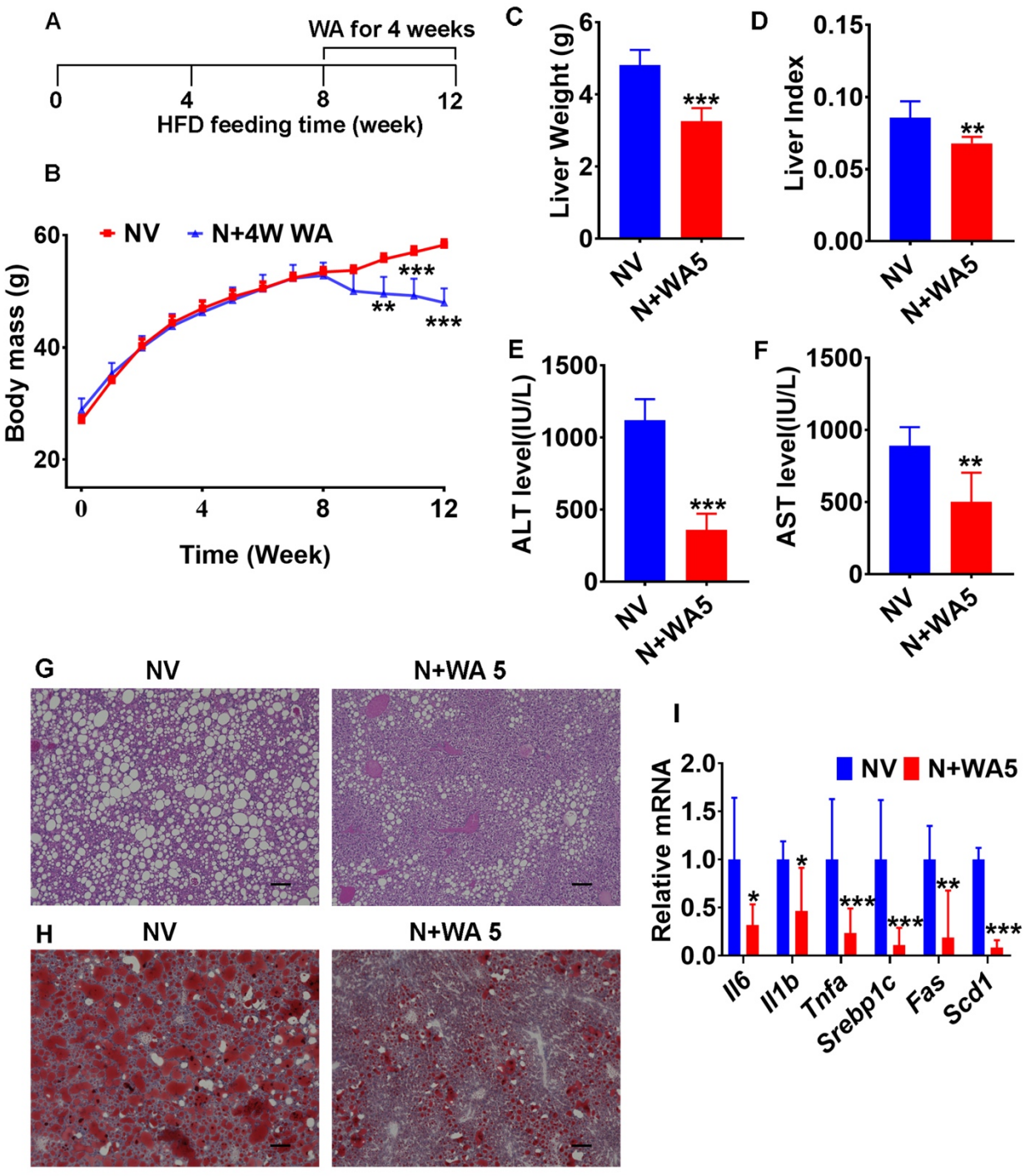

JPET Fast Forward. Published on August 16, 2019 as DOI: 10.1124/jpet.119.256792
This article has not been copyedited and formatted. The final version may differ from this version.

Figure 12

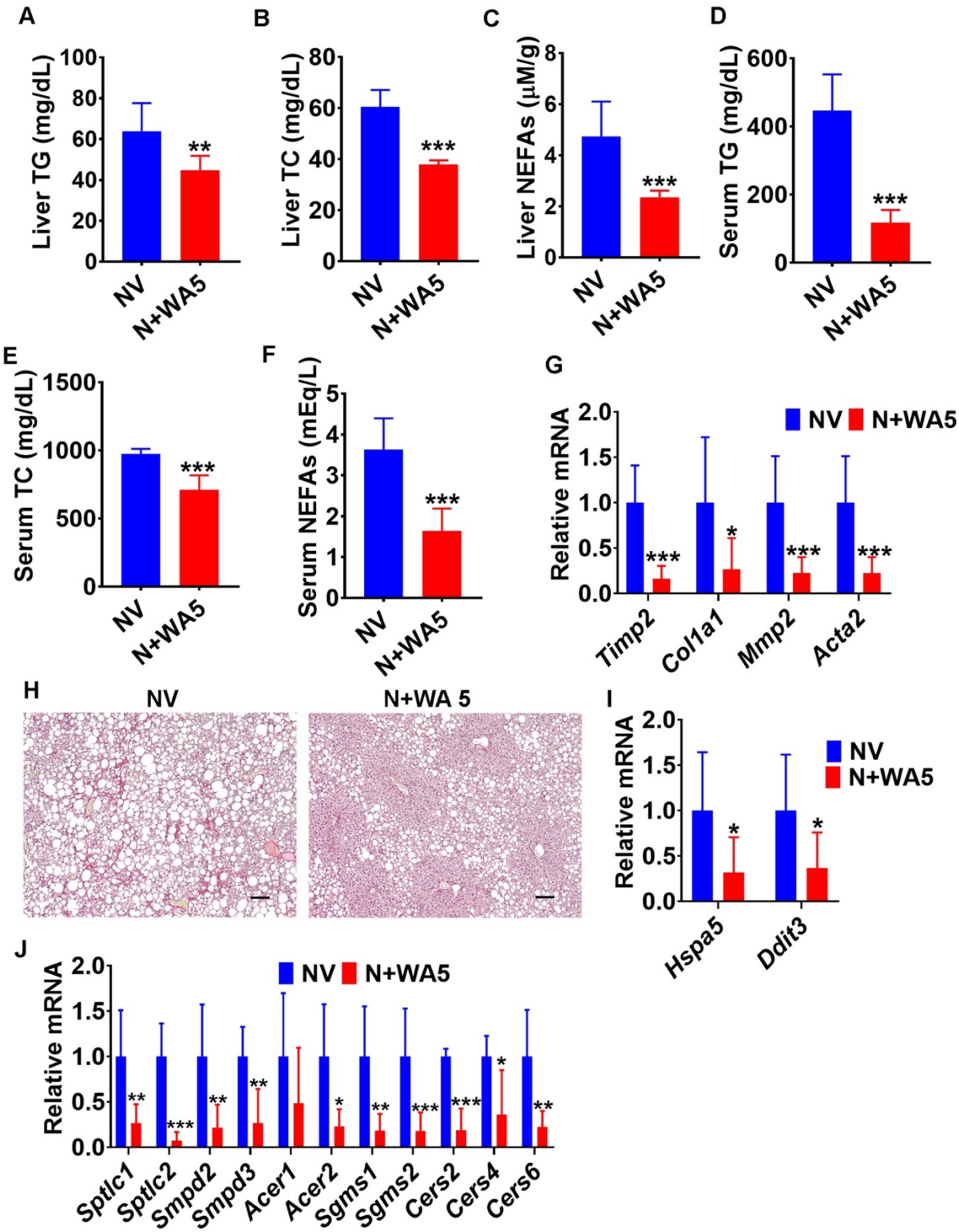

JPET Fast Forward. Published on August 16, 2019 as DOI: 10.1124/jpet.119.256792
This article has not been copyedited and formatted. The final version may differ from this version.

Figure 13